CHAPTER 19

Ribosomes and Transfer RNA

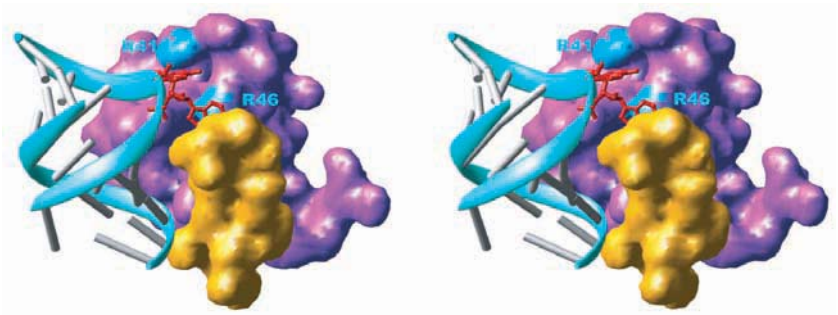

Stereo view of intimate association between 16S rRNA bases A1492 and A1493 (red stick structures) and pockets formed from IF1 (magenta) and S12 (yellow). *From Carter et al., Science 291: p. 500. © 2001 AAAS.*

In Chapter 3 we examined a few aspects of translation. We learned that ribosomes are the cell's protein factories and that transfer RNA plays a crucial adapter role, binding an amino acid at one end and an mRNA codon at the other. Chapters 17 and 18 expanded on the mechanisms of translation initiation, elongation, and termination, without dealing in depth with ribosomes and tRNA. Let us continue our discussion of translation with a closer look at these two essential agents.

19.1 Ribosomes

Chapter 3 introduced the *E. coli* ribosome as a two-part structure with a sedimentation coefficient of 70S. The two subunits of this structure are the **30S** and **50S** ribosomal subunits. We also learned in chapter 3 that the small subunit decodes the mRNA and the large subunit links amino acids together through peptide bonds. In this section we will focus on the bacterial ribosome, its overall structure, composition, assembly, and function.

Fine Structure of the 70S Ribosome

X-ray crystallography provides the best structural information but that is a difficult task with an asymmetric object as large as a ribosome. Despite the difficulty, Harry Noller and colleagues succeeded in obtaining crystals of ribosomes from the bacterium *Thermus thermophilus* that were suitable for x-ray crystallography. By 1999, they had obtained crystal structures of these ribosomes. These studies provided the most detailed structure to that time of the intact ribosome, at a resolution as great as 7.8 Å.

Then, in 2001 Noller and colleagues crystallized a complex of *T. thermophilus* 70S ribosomes plus an mRNA analog, and tRNAs bound to the P and E sites of the ribosome. These crystals yielded a structure at 5.5 Å resolution, a considerable improvement over the previous structure. These workers also crystallized these same complexes with and without tRNA bound to the A site and obtained the structure of the tRNA in the A site by difference, to a resolution of 7 Å.

Figure 19.1 shows the crystal structure of the 70S ribosome. Panels (a–d) show the ribosome in four different orientations: front, right side, back, and left side. The 16S rRNA of the 30S subunit is in cyan and the 30S proteins are in blue. The 23S rRNA of the 50S subunit is in gray, the 5S rRNA is in dark blue, and the 50S proteins are in purple. The tRNAs in the A, P, and E sites are in gold, orange, and red, respectively, although they are difficult to see in panels a–d because they lie in a cleft between the two ribosomal subunits. Most of the ribosomal proteins are identified. Notice L9 sticking out far to the side of the main body of the ribosome (to the left in panel [a]). Figure 19.1e shows a top view of the ribosome, in which the three tRNAs are clearly visible. Notice the anticodon stem-loops of all three pointing down into the 30S subunit at the bottom.

Panels f and g show the two subunits separated to reveal the positions of the tRNAs. The 30S particle has been rotated 180 degrees around its vertical axis so we can see the three tRNAs. Notice that the cleft where the tRNAs bind is lined mostly with rRNA in both subunits; the proteins are mostly peripheral in these views. This finding suggests that rRNAs, not proteins, dominate in the crucial interactions with tRNAs in decoding in the 30S subunit and peptide bond synthesis in the 50S subunit. Furthermore, the ribosome interacts with the conserved portions of all three t-RNAs, allowing it to bind in exactly the same way to all the different tRNAs it encounters.

Notice again in panel (g) the anticodon stem-loops pointing down into the 30S subunit. The anticodons of the tRNAs in the A and P sites approach each other within 10 Å, which does not seem close enough to allow them to bind to adjacent codons. The ribosome solves this problem by kinking the mRNA by 45 degrees between the codons in the A and P sites (Figure 19.2). This points the two codons in the proper directions to be decoded by the tRNAs. Figure 19.1f shows that the tRNAs in the A and P sites also approach each other closely in the 50S subunit. Although it is difficult to see in this view, the acceptor stems of these two tRNAs insert into the peptidyl transferase pocket in the 50S subunit and approach each other within 5 Å. This close approach is necessary because the amino acid and the peptide bound to these two tRNAs must join during peptide bond formation.

The 70S ribosomal crystal structure reveals 12 contacts between subunits (intersubunit bridges), which are illustrated in Figure 19.3. Most of these bridges consist of RNA, rather than protein. Indeed, all of the bridges near the tRNA-binding sites involve only RNA. Notice that bridges B2a, B3, B5, and B6, all involve a single helical domain (helix 44) of the 16S rRNA in the 30S subunit (see Figure 19.2). This helix is a major contributor to contact between the two subunits, and, as we will see later in this chapter, it also plays a role in codon–anticodon recognition. Because the translocation of tRNAs from A to P to E sites requires movement of 20–50 Å, it is very likely that at least some of the intersubunit bridges are dynamic, breaking and reforming to allow translocation to occur.

Figure 19.4 is a more schematic view of the ribosome that emphasizes three important points: First, a large cavity exists between the two ribosomal subunits that can accommodate the three tRNAs. Second, the tRNAs interact with the 30S subunit through their anticodon ends, which bind to the mRNA that is also bound to the 30S subunit. Third, the tRNAs interact with the 50S subunit through their acceptor stems. This makes sense because the acceptor stems must come together during the peptidyl transferase reaction, which takes place on the 50S subunit. During this reaction, the peptide, linked to the acceptor stem of the peptidyl-tRNA in the P site, joins the amino acid, linked to the acceptor stem of the aminoacyl-tRNA in the A site.

In 2005, Jamie Doudna Cate and colleagues achieved a major coup: They obtained the crystal structure of the *E. coli* 70S ribosome at 3.5-Å resolution. Not only was this the best resolution to date of any 70S ribosome, it was the long-sought structure of the *E. coli* ribosome, which is complemented by decades of biochemical and genetic data. Before this structure was available, scientists had to try to fit these biochemical and genetic data on the *E. coli*

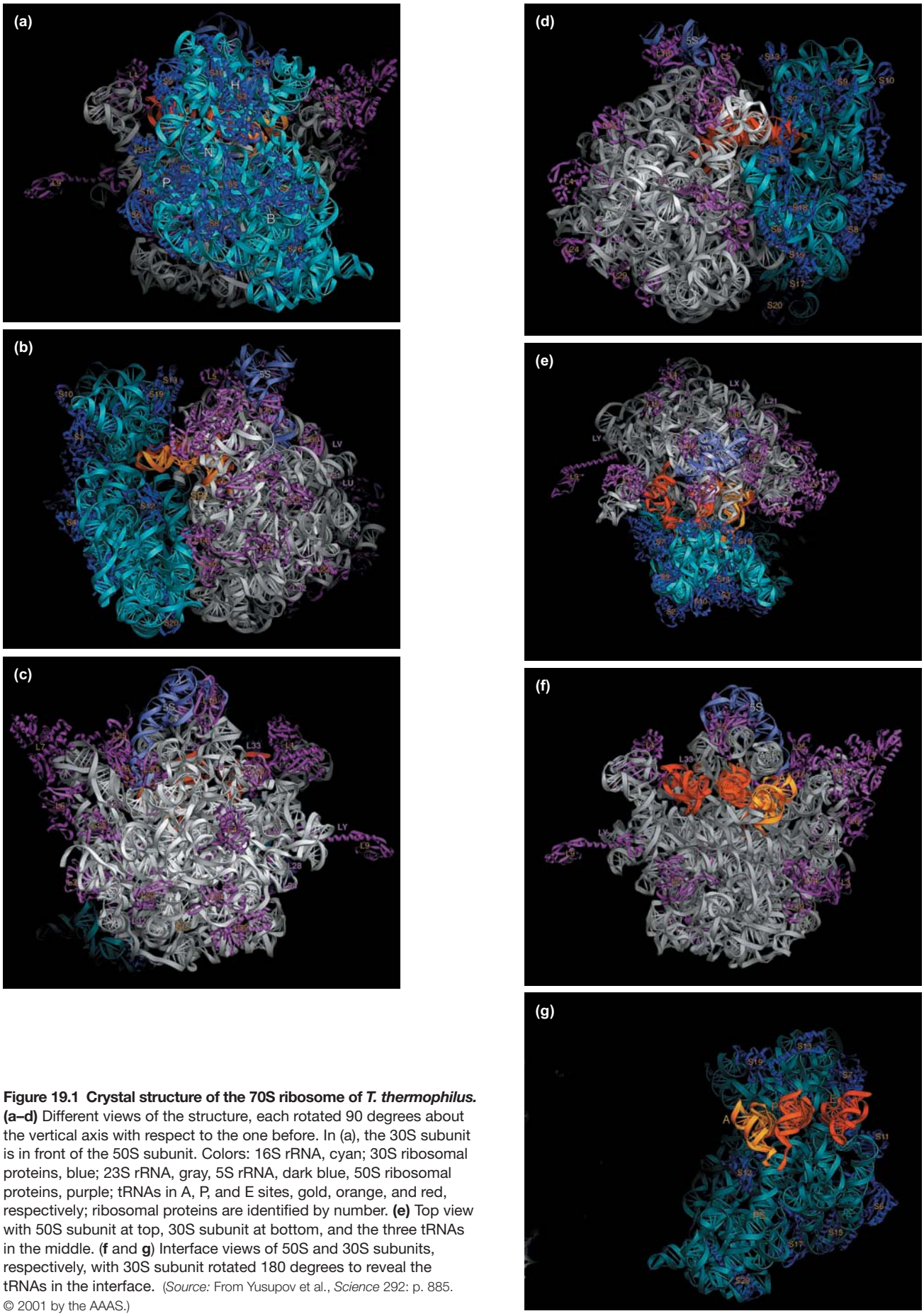

Figure 19.1 Crystal structure of the 70S ribosome of *T. thermophilus*. **(a–d)** Different views of the structure, each rotated 90 degrees about the vertical axis with respect to the one before. In (a), the 30S subunit is in front of the 50S subunit. Colors: 16S rRNA, cyan; 30S ribosomal proteins, blue; 23S rRNA, gray, 5S rRNA, dark blue, 50S ribosomal proteins, purple; tRNAs in A, P, and E sites, gold, orange, and red, respectively; ribosomal proteins are identified by number. **(e)** Top view with 50S subunit at top, 30S subunit at bottom, and the three tRNAs in the middle. (**f** and **g**) Interface views of 50S and 30S subunits, respectively, with 30S subunit rotated 180 degrees to reveal the tRNAs in the interface. (*Source:* From Yusupov et al., *Science* 292: p. 885.)

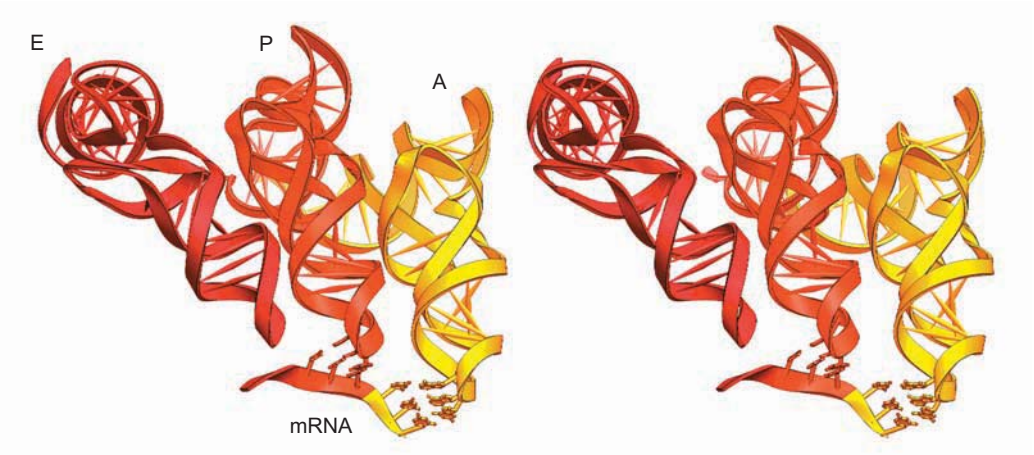

Figure 19.2 Stereo view of the codon–anticodon base-pairing in the A and P sites. All three tRNAs are shown, color-coded as in Figure 19.1 (A, gold; P, orange; and E, red). The bases of the codons and anticodons are shown as stick figures at bottom. Note the 45-degree kink in the mRNA between codons. The anticodon of the tRNA in the E site is not shown because it is not base-paired to mRNA. (*Source:* From Yusupov et al., *Science* 292: p. 893. © 2001 by the AAAS.)

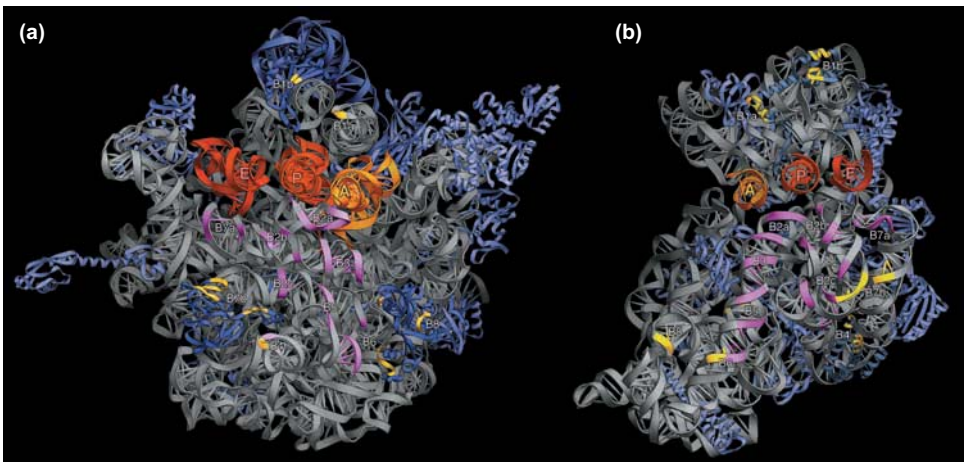

Figure 19.3 Interface view showing intersubunit bridges. (**a** and **b**) 50S and 30S subunits, respectively. In both subunits, large rRNAs are in gray, 5S rRNA is in dark blue at top of 50S particle, and proteins are in light blue. tRNAs are colored as in Figure 19.1 in gold, orange, and red. RNA–RNA bridges between subunits are in pink, and protein–protein bridges are in yellow. All bridges are numbered (B1a, B1b, B2a, etc.) (*Source:* From Yusupov et al., *Science* 292: p. 890. © 2001 by the AAAS.)

ribosome to the structure of a ribosome from another bacterium (*T. thermophilus*). That is probably a valid approach in most cases, but there are always doubts, especially because of the very different environments in which the two bacteria grow: mammalian intestines and boiling hot springs, respectively.

The latest structure contains a massive amount of data, and these data are not yet fully analyzed. Nevertheless, several interesting findings have emerged. Most strikingly, each unit cell of the crystal contained two different ribosomal structures, termed "ribosome I" and "ribosome II." The major differences between the two structures were due to rigid body motions of ribosomal domains. The most obvious of these motions was a rotation of the head of the 30S particle, 6 degrees toward the E site, from ribosome I to ribosome II. This rotation is even more pronounced (12 degrees toward the E site) when the *T. thermophilus* structure is compared to *E. coli* ribosome II.

This rotation of the head is almost certainly related to translocation of the mRNA and tRNAs through the ribosome. In fact, in 2000, Joachim Frank and Rajendra Kumar Agrawal had performed a cryo-electron microscopy study of ribosomes during translocation, and noted that the two subunits moved relative to each other. Furthermore, the mRNA channel widened during the process to allow the motion, then closed up again after translocation. Thus, the ribosome appears to act like a ratchet during translocation, and the rotation of the 30S particle head is probably part of this ratchet action.

Eukaryotic cytoplasmic ribosomes are more complex than bacterial ones. In mammals, the whole ribosome has a sedimentation coefficient of 80S and is composed of a 40S

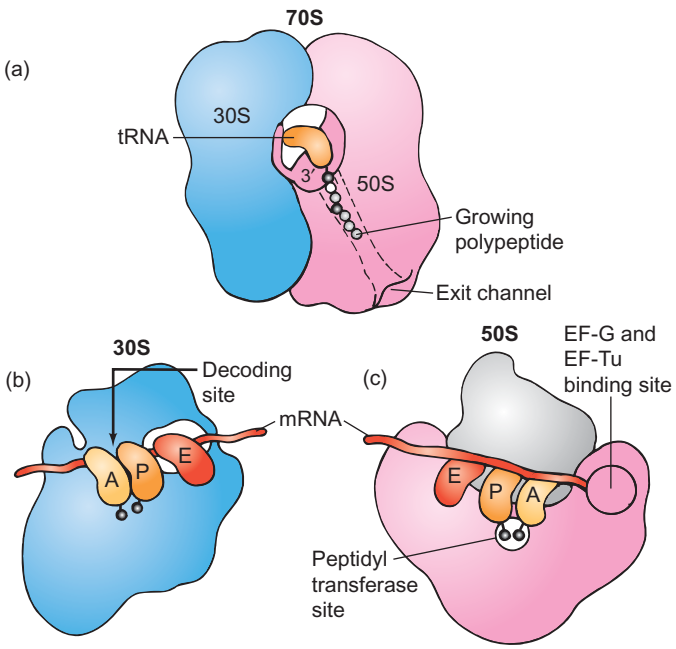

Figure 19.4 Schematic representation of the ribosome. **(a)** 70S ribosome, showing the large cavern between subunits, which can accommodate three tRNAs at a time. The peptidyl tRNA in the P site is shown, with the nascent polypeptide feeding through an exit tunnel in the 50S subunit. Notice that the interaction between the tRNA and the 30S subunit is through the tRNA's anticodon end, but the interaction between the tRNA and the 50S subunit is through the tRNA's acceptor stem. **(b)** The 30S subunit, with an mRNA and all three tRNAs bound. **(c)** The 50S subunit with an mRNA and all three tRNAs bound. (*Source:* Adapted from Liljas, A., Function is structure. *Science* 285:2078, 1999.)

and a 60S subunit. The 40S subunit contains one (18S) rRNA, and the 60S subunit contains three (28S, 5.8S, and 5S) rRNAs. Budding yeast ribosomes contain 79 ribosomal proteins, compared to 55 in *E. coli*. Eukaryotic organelles also have their own ribosomes, but these are less complex. In fact, they are even simpler than bacterial ribosomes.

SUMMARY The crystal structure of the *T. thermophilus* 70S ribosome in a complex with an mRNA analog and three tRNAs reveals the following: The positions and tertiary structures of all three rRNAs and most of the proteins can be determined. The shapes and locations of tRNAs in the A, P, and E sites are evident. The binding sites for the tRNAs in the ribosome are composed primarily of rRNA, rather than protein. The anticodons of the tRNAs in the A and P sites approach each other closely enough to base-pair with adjacent codons bound to the 30S subunit, given that the mRNA kinks 45 degrees between the two codons. The acceptor stems of the tRNAs in the A and P sites also approach each other closely—within just 5 Å—in the peptidyl transferase pocket in the 50S subunit. This is consistent with the need for the two stems to interact during peptide bond formation. Twelve contacts between subunits can be seen, and most of these are mediated by RNA–RNA interactions.

The crystal structure of the *E. coli* ribosome contains two structures that differ from each other by rigid body motions of domains of the ribosome, relative to each other. In particular, the head of the 30S particle rotates by 6 degrees, and by 12 degrees compared to the *T. thermophilus* ribosome. This rotation is probably part of the ratchet action of the ribosome that occurs during translocation.

Eukaryotic cytoplasmic ribosomes are larger and more complex than their prokaryotic counterparts, but eukaryotic organellar ribosomes are smaller than prokaryotic ones.

Ribosome Composition

We learned in Chapter 3 that the *E. coli* 30S ribosomal subunit is composed of a molecule of 16S rRNA and 21 ribosomal proteins, whereas the 50S particle contains two rRNAs (5S and 23S) and 34 ribosomal proteins. The rRNAs were relatively easy to purify by phenol extracting ribosomes to remove the proteins, leaving rRNA in solution. Then the sizes of the rRNAs could be determined by ultracentrifugation.

On the other hand, the ribosomal proteins are much more complex mixtures and had to be resolved by finer methods. The 30S ribosomal proteins can be displayed by one-dimensional SDS-PAGE to reveal a number of different bands ranging in mass from about 60 down to about 8 kD, but some of the proteins are incompletely resolved by this method. In 1970, E. Kaldschmidt and H.G. Wittmann used two-dimensional gel electrophoresis to give almost complete resolution of the ribosomal proteins from both subunits. In this version of the technique, the two steps were simply native PAGE (no SDS) performed at two different pH values and acrylamide concentrations.

Figure 19.5 depicts the results of two-dimensional electrophoresis on *E. coli* 30S and 50S proteins. Each spot contains a protein, identified as S1–S21 for the 30S proteins, and L1–L33 (L34 is not visible) for the 50S proteins. The S and L stand for small and large ribosomal subunits. The numbering starts with the largest protein and ends with the smallest. Thus, S1 is about 60 kD and S21 is about 8 kD. You can see almost all the proteins, and almost all of them are resolved from their neighbors.

Eukaryotic ribosomes are more complex. The mammalian 40S subunit contains an 18S rRNA and about 30 proteins. The mammalian 60S subunit holds three rRNAs (5S, 5.8S, and 28S) and about 40 proteins. As we learned in

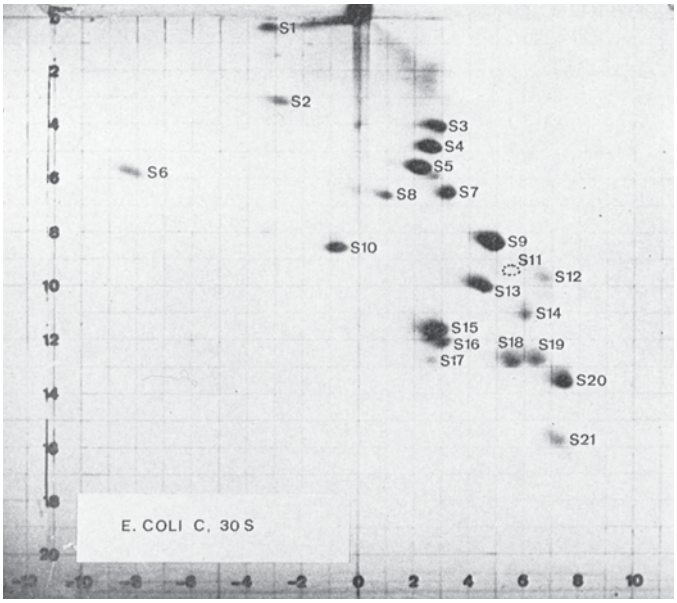

(a)

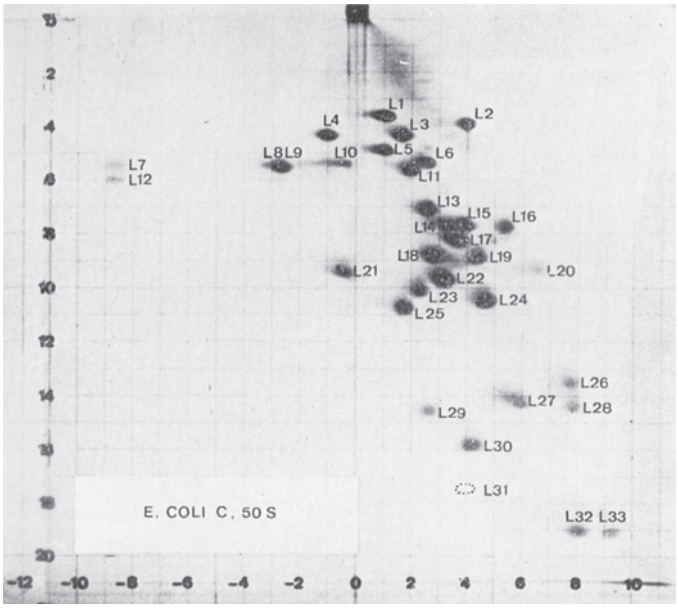

(b)

Figure 19.5 Two-dimensional gel electrophoresis of proteins from (a) *E. coli* 30S subunits and (b) *E. coli* 50S subunits. Proteins are identified by number, with S designating the small ribosomal subunit, and L, the large subunit. Electrophoresis in the first dimension (horizontal) was run at pH 8.6 and 8% acrylamide; electrophoresis in the second dimension (vertical) was run at pH 4.6 and 18% acrylamide. Proteins S11 and L31 were not visible on these gels, but their positions from other experiments are marked with dotted circles. (*Source:* Kaltschmidt, E. and H.G. Wittmann, Ribosomal proteins XII: Number of proteins in small and large ribosomal subunits of *Escherichia coli* as determined by two-dimensional gel electrophoresis. *Proceedings of the National Academy of Sciences USA* 67 (1970) f. 1–2, pp. 1277–78.)

Chapters 10 and 16, the 5.8S, 18S, and 28S rRNAs all come from the same transcript, made by RNA polymerase I, but the 5S rRNA is made as a separate transcript by RNA polymerase III. Eukaryotic organellar rRNAs are even smaller than their prokaryotic counterparts. For example, the mammalian mitochondrial small ribosomal subunit has an rRNA with a sedimentation coefficient of only 12S.

SUMMARY The *E. coli* 30S subunit contains a 16S rRNA and 21 proteins (S1–S21). The 50S subunit contains a 5S rRNA, a 23S rRNA, and 34 proteins (L1–L34). Eukaryotic cytoplasmic ribosomes are larger and contain more RNAs and proteins than their prokaryotic counterparts.

Fine Structure of the 30S Subunit

As soon as the sequences of the *E. coli* rRNAs became known, molecular biologists began proposing models for their secondary structures. The idea is to find the most stable molecule—the one with the most intramolecular base pairing. Figure 19.6 depicts a consensus secondary structure for the 16S rRNA that has been verified by x-ray crystallography of 30S ribosomal subunits. Note the extensive base pairing proposed for this molecule. Note also how the molecule can be divided into three almost independently folded domains (one of which has two subdomains), highlighted in different colors.

How does the three-dimensional arrangement of the 16S rRNA relate to the positions of the ribosomal proteins in the intact ribosomal subunit? The best way to obtain such information is to perform x-ray crystallography, and V. Ramakrishnan and colleagues succeeded in 2000 in solving the crystal structure for the *T. thermophilus* 30S subunit to a resolution of 3.0 Å. At almost the same time, a group led by François Franceschi determined the same structure to 3.3 Å resolution. The structure of Ramakrishnan and colleagues contained all of the ordered regions of the 16S rRNA (over 99% of the RNA molecule) and of 20 ribosomal proteins (95% of the protein). The parts of the proteins missing from the structure were only at their disordered ends.

Figure 19.7a is a stereo diagram of the 16S rRNA alone, and the RNA clearly outlines all of the important parts of the ribosome, including the head, platform, and body. In addition, we can see a neck joining the head to the body, a beak (sometimes called a nose) protruding to the left from the head, and a spur at the lower left of the body. The color coding is the same as in Figure 19.6, emphasizing the fact that the 16S rRNA secondary structural elements correspond to independent three-dimensional elements. Figure 19.7b shows front and back views of the 30S subunit with proteins added to the RNA. The proteins do not cause major changes in the overall shape of the subunit. In other words,

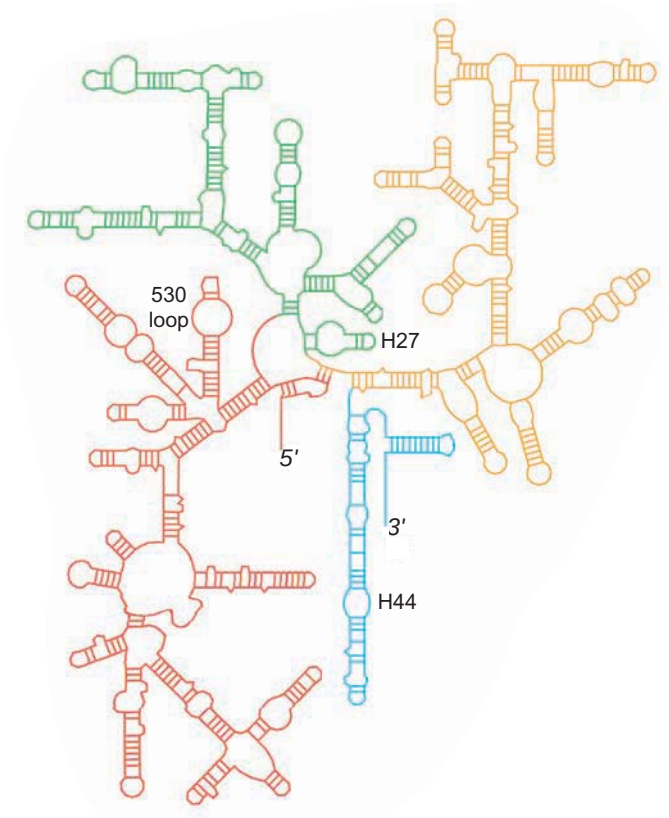

Figure 19.6 Secondary structure of 16S rRNA. This structure is based on optimal base-pairing and on x-ray crystallography of 30S ribosomal subunits from *T. thermophilus.* Two helices (H27 and H44) and the 530 loop, discussed later in the chapter, are labeled. Red, 5′-domain; green, central domain; yellow, 3′-major domain; turquoise, 3′-minor domain. (*Source:* Adapted from Wimberly, B.T., D.E. Brodersen, W.M. Clemons Jr., R.J. Morgan-Warren, A.P. Carter, C. Vonrhein, T. Hartsch, and V. Ramakrishnan, Structure of the 30S ribosomal subunit. *Nature* 407 (21 Sep 2000) f. 2a, p. 329.)

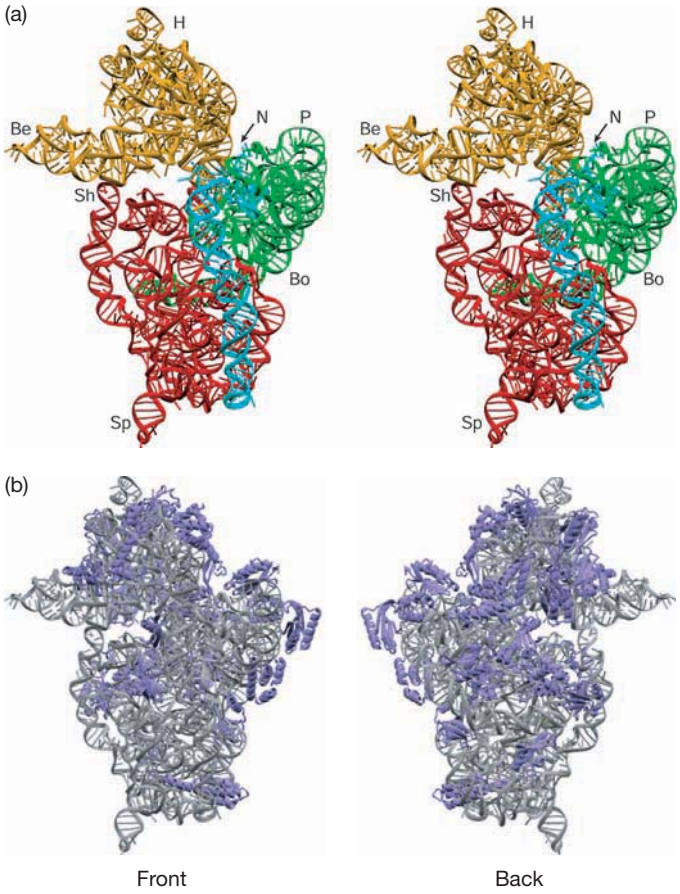

Figure 19.7 Crystal structure of the 30S ribosomal subunit. **(a)** Stereo diagram of the 16S rRNA portion of the 30S subunit from *T. thermophilus.* The major features are identified as follows: H, head; Be, beak; Sh, shoulder; N, neck; P, platform; Bo, body; and Sp, spur. Colors have the same meaning as in Figure 19.6. **(b)** Front and back views of the 30S subunit with the proteins (purple) added to the RNA (gray). The front is conventionally recognized as the side of the 30S subunit that interacts with the 50S subunit. Note that these are two different views of the ribosome, not a stereo diagram. (*Source:* Wimberly, B.T., D.E. Brodersen, W.M. Clemons Jr., R.J. Morgan-Warren, A.P. Carter, C. Vonrhein, T. Hartsch, and V. Ramakrishnan, Structure of the 30S ribosomal subunit. *Nature* 407 (21 Sep 2000) f. 2b, p. 329. Copyright © Macmillan Magazines Ltd.)

the proteins do not contribute exclusively to any of the major parts of the subunit. These statements do not mean that the 16S rRNA would take the shape shown here in the absence of proteins, just that the rRNA is such a major part of the 30S subunit that its shape in the intact subunit resembles a skeleton of the subunit itself. The locations of most of the proteins agree well with the locations determined earlier by other methods.

SUMMARY Sequence studies of 16S rRNA led to a proposal for the secondary structure (intramolecular base pairing) of this molecule. X-ray crystallography studies have confirmed the conclusions of these studies. They show a 30S subunit with an extensively base-paired 16S rRNA whose shape essentially outlines that of the whole particle. The x-ray crystallography studies have also confirmed the locations of most of the 30S ribosomal proteins.

Interaction of the 30S Subunit with Antibiotics Ramakrishnan and colleagues also obtained the crystal structures of the 30S subunit bound to three different antibiotics: spectinomycin, which inhibits translocation; streptomycin, which causes errors in translation; and paromomycin, which increases the error rate by another mechanism. These data, together with the structure of the 30S subunit by itself, gave further insights about the mechanism of translation.

First, Ramakrishnan and coworkers superimposed on their 30S subunit structure the positions of the three aminoacyl-tRNAs from the structure of the whole 70S ribosome (recall Figure 19.1). Figure 19.8a and b show two different views of the positions of the anticodon stem loops

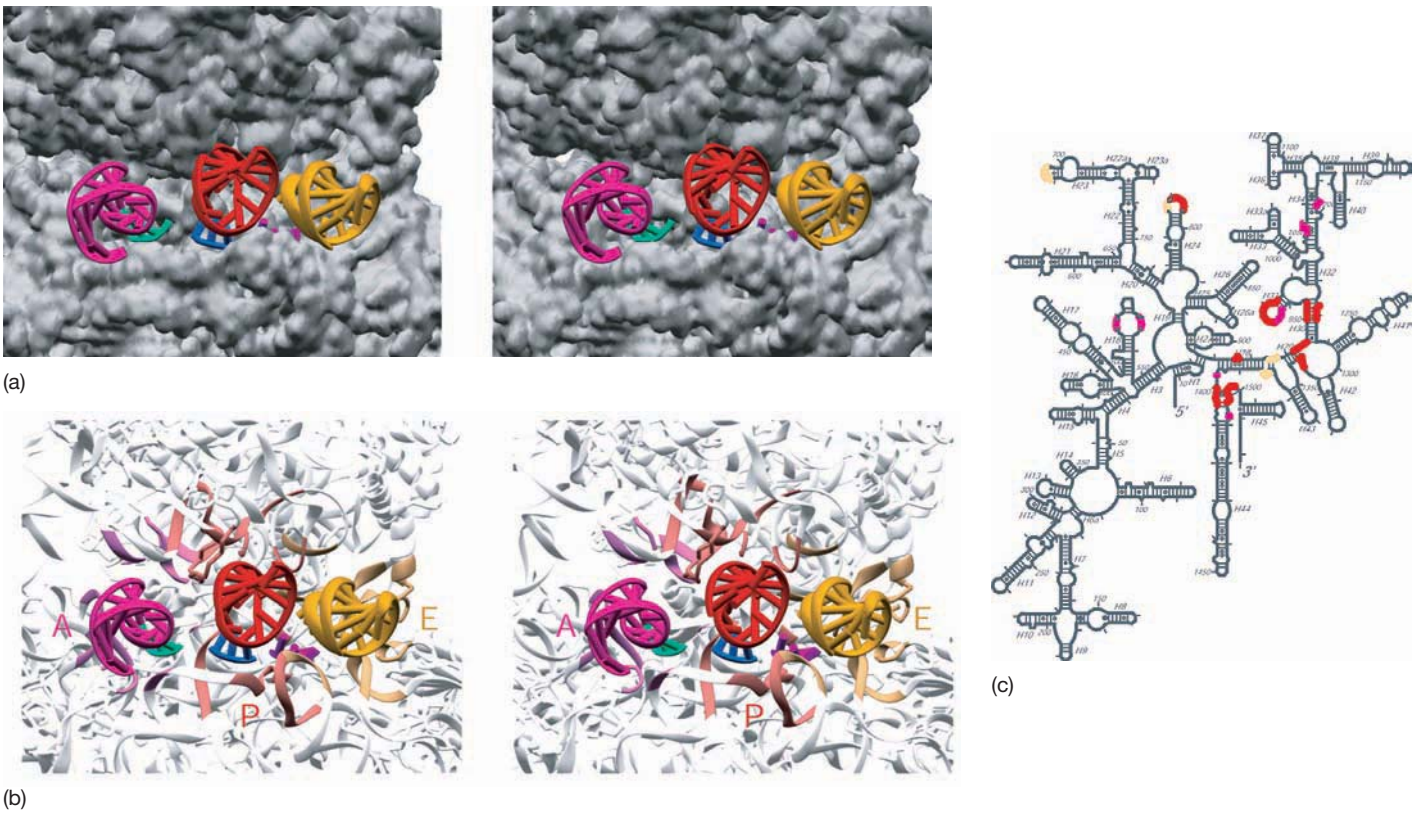

Figure 19.8 Locations of the A, P, and E sites on the 30S ribosomal subunit. (a) and **(b)** Two different stereo views of the inferred placement of the anticodon stem-loops and mRNA codons on the 30S ribosomal subunit. The anticodon stem-loops are colored magenta (A site), red (P site), and gold (E site). The mRNA codons are colored green (A site) blue, (P site), and dotted magenta (E site). **(c)** Secondary structure of the 16S rRNA showing the regions involved in each of the three sites, color-coded the same as the anticodon stem-loops in parts (a) and (b): magenta, A site; red, P site; and gold, E site. (*Source:* Carter, A.P., W.M. Clemons Jr., D.E. Brodersen, R.J. Morgan-Warren, B.T. Wimberly, and V. Ramakrishnan, Functional insights from the structure of the 30S ribosomal subunit and its interactions with antibiotics. *Nature* 407 (21 Sep 2000) f. 1, p. 341. Copyright © MacMillan Magazines Ltd.)

of the aminoacyl-tRNAs, and codons of a hypothetical mRNA, bound to the A, P, and E sites on the 30S subunit. It is striking that the codons and anticodons in the A and P sites lie in a region near the neck of the 30S subunit that is almost devoid of protein. Thus, codon–anticodon recognition occurs in an environment that is surrounded by segments of the 16S rRNA, and very little protein. Figure 19.8c shows which parts of the 16S rRNA are involved at each of the three sites.

The positions of the three antibiotics on the 30S subunit help elucidate the two activities of the 30S subunit: translocation and **decoding** (codon–anticodon recognition). The geometry of the 30S subunit suggests that translocation must involve movement of the head relative to the body. **Spectinomycin** is a rigid three-ring molecule that inhibits translocation. Its binding site on the 30S subunit lies near the point around which the head presumably pivots during translocation. Thus, it is in position to block the turning of the head that is necessary for translocation.

Streptomycin increases the error rate of translation by interfering with initial codon–anticodon recognition and with proofreading. The position of streptomycin on the 30S subunit (Figure 19.9) provides some clues about how this antibiotic works. Streptomycin lies very close to the A site, where decoding occurs. In particular, it makes a close contact with A913 in helix H27 of the 16S rRNA.

This placement of streptomycin is significant because the H27 helix is thought to have two alternative base-pairing patterns during translation, and these patterns affect accuracy. The first is called the ***ram*** state (from **ribosome ambiguity**). As its name implies, this base-pairing scheme for H27 stabilizes interactions between codons and anticodons, even noncognate anticodons, so accuracy is low in the *ram* state. (The crystal structures obtained by Ramakrishnan and colleagues contain the H27 helix in the *ram* state.) The alternative base-pairing pattern is **restrictive,** and it demands accurate pairing between codon and anticodon. If the ribosome is locked into the *ram* state it accepts noncognate aminoacyl-tRNAs too readily and cannot switch to the restrictive state required for proofreading. As a result, translation is inaccurate. On the other hand, if the ribosome is locked into the restrictive state,

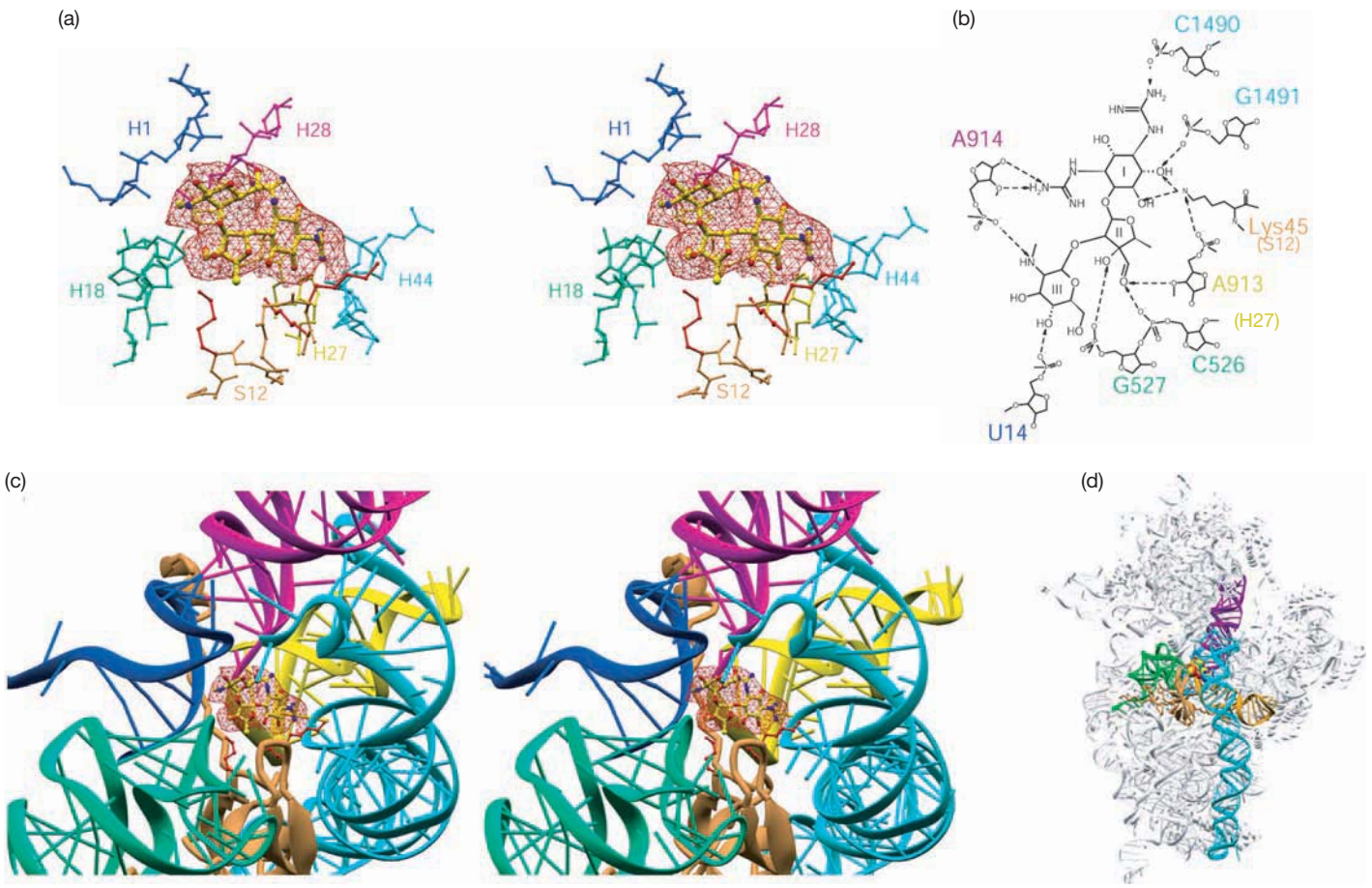

Figure 19.9 Interaction of streptomycin with the 30S ribosomal subunit. (a) Stereo diagram of streptomycin and its nearest neighbors in the 30S subunit. The streptomycin molecule is shown as a ball-and-stick model within a cage of electron density (actually the difference in density between 30S subunits with and without the antibiotic). The nearby helices of the 16S rRNA are shown. Notice especially the H27 helix (yellow), which is crucial for the activity of this antibiotic. Notice also the position of the only protein near the A site—S12 (tan and red), which is also important in streptomycin activity. Amino acids of S12 that are altered in streptomycin-resistant cells are shown in red. **(b)** Interactions of specific groups of streptomycin (containing rings numbered I, II, and III) with neighboring atoms on the 30S subunit. Notice the interactions with A913 of H27 and Lys45 of S12. **(c)** Another stereo view of streptomycin and its nearest neighbors. Color coding is the same as in panel (a). Notice again H27 (yellow) and S12 (tan). **(d)** Location of the streptomycin-binding site on the whole 30S subunit. Streptomycin is shown as a small, red space-filling model at the point where all the colored 16S rRNA helices converge. (*Source:* Carter, A.P., W.M. Clemons Jr., D.E. Brodersen, R.J. Morgan-Warren, B.T. Wimberly, and V. Ramakrishnan, Functional insights from the structure of the 30S ribosomal subunit and its interactions with antibiotics. *Nature* 407 (21 Sep 2000) f. 5, p. 345. Copyright © Macmillan Magazines Ltd.)

it is hyperaccurate—it rarely makes mistakes, but aminoacyl-tRNAs have a difficult time binding to the A site, so translation is inefficient.

The interactions between streptomycin and the 30S subunit indicate the antibiotic stabilizes the *ram* state. This would reduce accuracy in two ways. First, it would favor the *ram* state during decoding and thereby encourage pairing between a codon and noncognate aminoacyl-tRNAs. Second, it would inhibit the switching to the restrictive state that is necessary for proofreading.

Mutations in the ribosomal protein S12 can confer streptomycin resistance or even streptomycin dependence. Almost all of these S12 mutations are in regions of the protein that stabilize the 908–915 part of H27 and the 524–527 part of H18. These are also parts of the 16S rRNA that stabilize the *ram* state. These considerations led Ramakrishnan and colleagues to propose the following two-part hypothesis: First, S12 mutations that cause streptomycin resistance destabilize the *ram* state enough to counteract the *ram* state stabilization produced by the antibiotic. The result is a ribosome that works properly even in the presence of streptomycin. Second, S12 mutations that cause streptomycin dependence destabilize the *ram* state so much that the mutant ribosomes need the antibiotic to confer normal stability to the *ram* state. The result is a ribosome that cannot carry out normal translation without streptomycin.

In other words, translation that is both accurate and efficient depends on a balance between the *ram* state and the restrictive state of the ribosome. Streptomycin can

tip the balance toward inaccuracy and efficiency by favoring the *ram* state, and mutations in S12 can tip the balance toward accuracy and inefficiency by favoring the restrictive state.

Paromomycin also decreases accuracy of translation by binding to the A site. In 2000, Ramakrishnan and coworkers showed that this antibiotic binds in the major groove of the H44 helix and "flips out" bases **A1492** and **A1493.** That is, it forces these bases out of the major helical groove and puts them in position to interact with the minor groove between the codon and anticodon in the A site. Bases A1492 and A1493 are universally conserved and are absolutely required for translation activity. Mutations in either of these two bases are lethal.

These factors led to the following hypothesis: During normal decoding, bases A1492 and A1493 flip out and form H bonds with the 2′-OH groups of the sugars in the minor groove of the short double helix formed by the codon–anticodon base pairs in the A site. This helps to stabilize the interaction between codon and anticodon, which is important because the three base pairs would otherwise provide little stability. Flipping these two bases out ordinarily requires energy but paromomycin eliminates this energy requirement by forcing the bases to flip out. In this way, paromomycin stabilizes binding of aminoacyl-tRNAs, including noncognate aminoacyl-tRNAs, to the A site and thereby increases the error rate.

No codon or anticodon were present in the crystal structure of the 30S subunit with paromomycin, so there was no direct evidence for the proposed interactions between bases A1492 and A1493 on the one hand, and the minor groove of the codon–anticodon duplex on the other.

In 2001, Ramakrishnan and coworkers provided direct evidence for their hypothesis. They soaked crystals of *T. thermophilus* 30S ribosomal subunits in a solution containing a 17-nt oligonucleotide corresponding to the anticodon stem-loop of $tRNA^{Phe}$, plus a U_6 oligonucleotide that codes for diphenylalanine. These molecules were both small enough to insert into their proper locations on the 30S subunit, mimicking the anticodon and codon of a full aminoacyl-tRNA and an mRNA, respectively.

Figure 19.10 shows stereo views of selected parts of the crystal structure of this complex. Panel (a) shows clearly that A1493 of helix H44 contacts the 2′-hydroxyl groups of the sugars of both nucleotides in the minor groove of the first codon–anticodon base pair (U1–A36). Panel (b) shows the less favorable interactions with A1493 if A36 of the anticodon is replaced by G. In panel (c), A1492 of helix H44 and G530 of the 530 loop of the 16S rRNA contact the 2′-hydroxyl groups of the sugars of both nucleotides in the second codon–anticodon base pair (U2–A35). These are the two most important base pairs in decoding, and both are stabilized by the flipped-out bases A1492 and A1493, in addition to some other ribosomal elements.

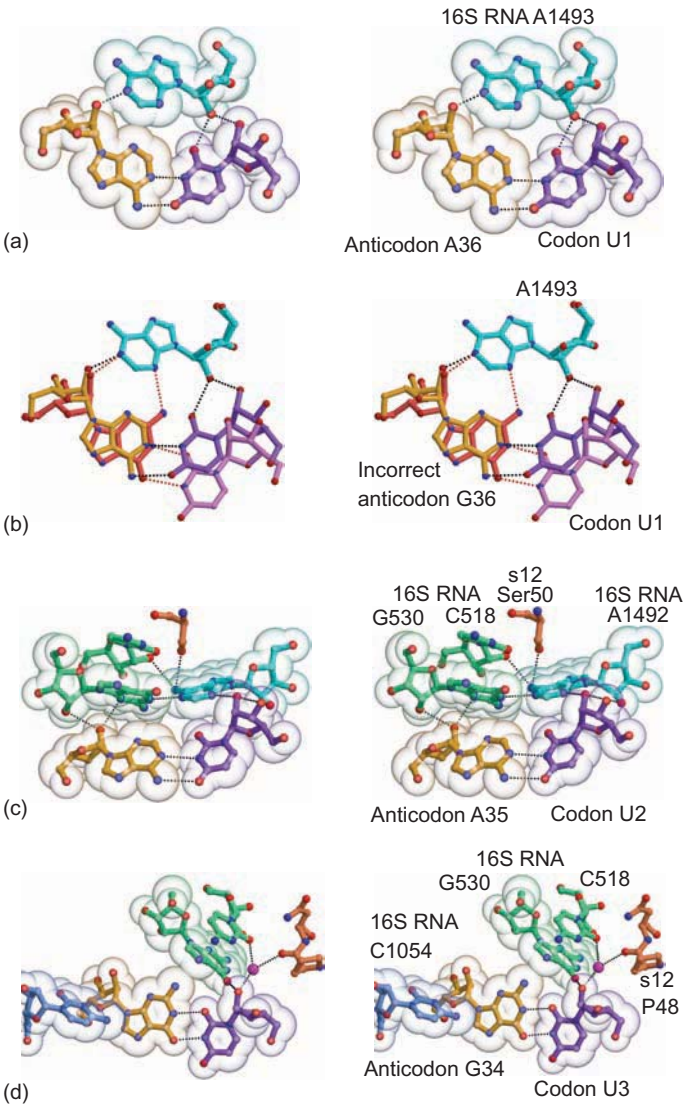

Figure 19.10 Stereo views of interactions between codon-anticodon base pairs and elements of the 30S ribosomal subunit. (a) A1493 of helix H44 binding in the minor groove of the U1-A36 base pair. **(b)** Same as in panel (a), but also showing the result of replacing A36 in the anticodon with G, so a wobble G–U pair forms between G36 and U1. Now the positions of G36 (red) and U1 (lavender) can be contrasted with the normal positions of A36 (gold) and U1 (purple). Notice that U1 has been displaced such that it loses its normal interactions with A1493 (represented by a black dotted line). This destabilizes the interaction and helps the ribosome discriminate between a cognate A-U anticodon-codon base pair and a noncognate G–U anticodon-codon base pair involving the first base in the codon. **(c)** A1492 and G530 binding in the minor groove of the U2-A35 base pair. **(d)** The wobble base pair U3-G34 interacts through U3 with G530, and, through a Mg^{2+} ion (magenta sphere), with C518 and proline 48 of protein S12. Base C1054 of the 16S rRNA stacks next to G34. (*Source:* From Ogle et al., *Science* 292: p. 900. © 2001 by the AAAS.)

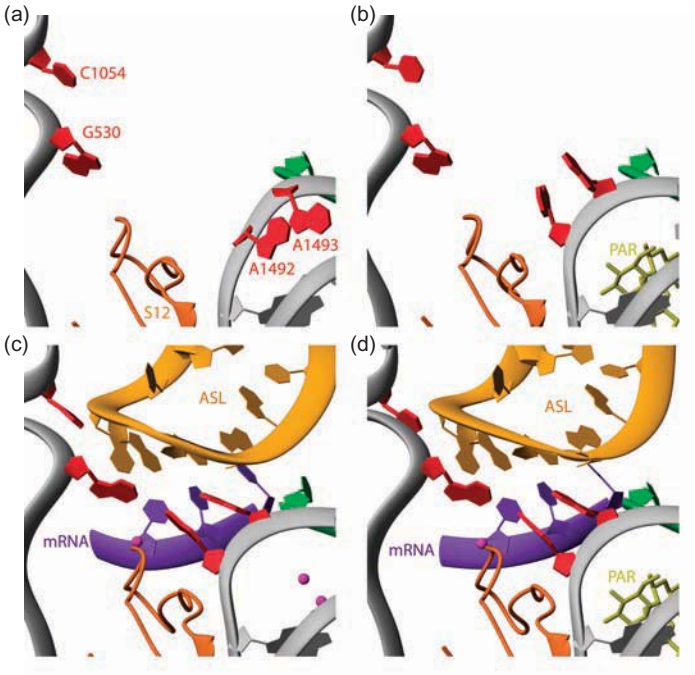

Figure 19.11 Structure of the decoding center in the presence and absence of tRNA, mRNA, and paromomycin. **(a)** The decoding center by itself. Note the positions of A1492 and A1493 in the H44 helix. The positions of these bases are very flexible. **(b)** The decoding center in the presence of paromomycin. Binding of the antibiotic inside helix H44 has forced A1492 and A1493 to positions outside the helix and into the decoding center. **(c)** The decoding center in the presence of mRNA and the anticodon stem loop (ASL) of the decoding center tRNA. A1492 and A1493 assume the same position in the decoding center that they would in the presence of paromomycin alone. **(d)** Same as in panel (c) except that paromomycin is present. The antibiotic makes little difference because A1492 and A1493 are already interacting in the decoding center. (*Source:* From Ogle et al., *Science* 292: p. 900. © 2001 by the AAAS.)

The third codon–anticodon base pair (wobble pair U3–G34, panel d) is also stabilized by ribosomal elements, including P48 of ribosomal protein S12 and G530 of 16S rRNA, but not by A1492 and 1493.

Figure 19.11 summarizes what these crystal structures tell us about the roles of A1492, A1493, and paromomycin in decoding. Comparing panels (a) and (b), we can see that paromomycin binds inside helix H44 and forces A1492 and A1493 out of the helix into the **decoding center** of the A site. Panel (c) illustrates decoding in the absence of paromomycin, and shows that A1492 and A1493 occupy the same positions as with paromomycin, and that these two rRNA bases are in perfect position to sense the fit between the bases in the first and second base pairs by feeling the positions of the ribose sugars in the minor groove of the codon–anticodon double helix. Indeed, A1492 and A1493, together with G530, are the key components of the decoding center of the ribosome. Panel (d) illustrates the same structure in the presence of paromomycin and again shows little change from the structure without the antibiotic.

All of these findings are consistent with the hypothesis that paromomycin, by nudging A1492 and A1493 out of helix H44, pays part of the energy cost of the induced fit between codon and anticodon at the decoding center. By so doing, the antibiotic makes base pairing between noncognate codons and anticodons easier, thereby increasing the frequency of mRNA misreading.

SUMMARY The 30S ribosomal subunit plays two roles. It facilitates proper decoding between codons and aminoacyl-tRNA anticodons, including proofreading. It also participates in translocation. Crystal structures of the 30S subunit with three antibiotics that interfere with these two roles shed light on translocation and decoding. Spectinomycin binds to the 30S subunit near the neck, where it can interfere with the movement of the head that is required for translocation. Streptomycin binds near the decoding center of the 30S subunit and stabilizes the *ram* state of the ribosome. This reduces fidelity of translation by allowing noncognate aminoacyl-tRNAs to bind relatively easily to the decoding center and by preventing the shift to the restrictive state that is necessary for proofreading. Paromomycin binds in the major groove of the 16S rRNA H44 helix near the decoding center. This flips out bases A1492 and A1493, so they can stabilize base pairing between codon and anticodon. This flipping-out process normally requires energy, but paromomycin forces it to occur and keeps the stabilizing bases in place. This state of the decoding center stabilizes codon–anticodon interaction, including interaction between noncognate codons and anticodons, so fidelity declines.

Interaction of the 30S Subunit with Initiation Factors We have seen in Chapter 17 that IF1 helps the other initiation factors do their jobs. Another postulated role of IF1 is to prevent aminoacyl-tRNAs from binding to the ribosomal A site until the initiation phase is over. This blockage of the A site presumably plays two roles. First, until the 50S particle joins the initiation complex, EF-Tu-directed proofreading of the aminoacyl-tRNA in the A site cannot occur. Thus, blockage of the A site prevents such inaccurate binding of aminoacyl-tRNAs and thereby promotes fidelity of translation. Second, it ensures that the initiator aminoacyl-tRNA binds to the P site, not the A site.

Ramakrishnan and coworkers have determined the crystal structure of IF1 bound to *T. thermophilus* 30S ribosomal subunits. The structure, presented in Figure 19.12b and c shows clearly that IF1 binds to and occludes the A site of the 30S subunit. It occupies much of the spot to which the tRNA would bind in the A site.

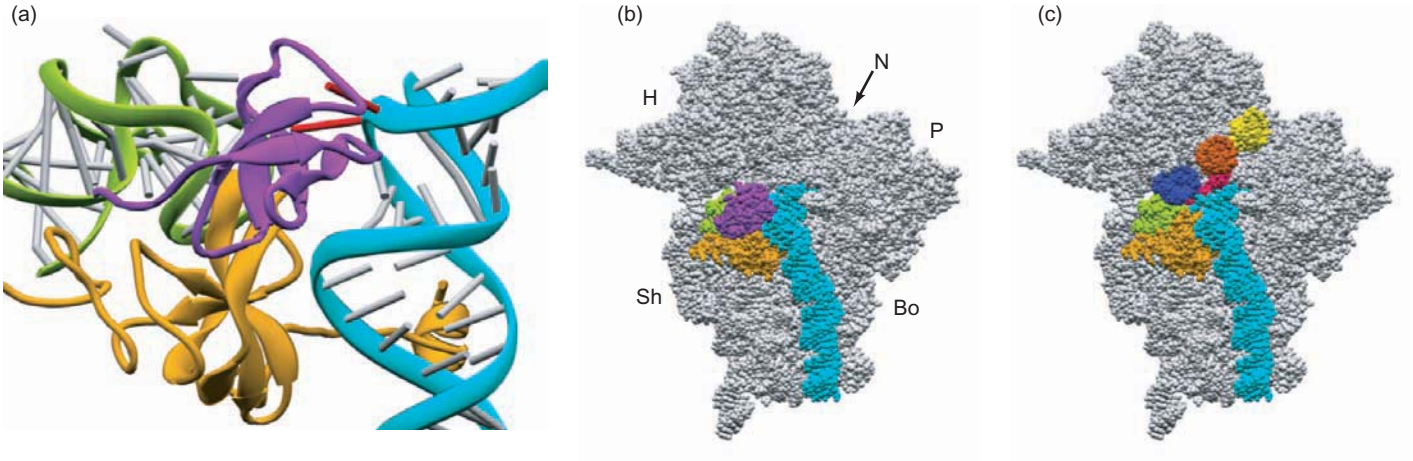

Figure 19.12 Crystal structure of the IF1–30S ribosomal subunit complex. (a) Close-up view showing IF1 in magenta, helix H44 of the 16S rRNA in turquoise (with A1492 and A1493 as red sticks), the 530 loop of the 16S rRNA in green, and the S12 protein in orange. **(b)** Overall view of the complex, with the same colors as in panel (a). The rest of the 30S subunit is in gray. **(c)** Overall view minus IF1, showing the positions of tRNAs in the A site (purple), P site (burnt orange), and E site (yellow-green). The other colors are as in panel (a). Notice the overlap between the tRNA in the A site and the position of IF1 in panel (a). (*Source:* From Carter et al., *Science* 291: p. 500. © 2001 by the AAAS.)

The crystals in this study did not include IF2, but we know from Chapter 17 that IF1 aids IF2 in binding fMet-tRNA to the P site, and it is also known that IF1 and IF2 interact. Thus, it is quite possible that binding of IF1 to the A site allows IF1 to help IF2 bind to the 30S subunit in such a way as to facilitate the binding of fMet-tRNA to the P site.

Experiments in the early 1970s appeared to show that IF1 facilitates the dissociation of the two ribosomal subunits. Actually, it also helps the two subunits reassociate, so it does not change the equilibrium between the two. It is only with the help of IF3, which prevents reassociation, that IF1 appears to be an agent of ribosomal dissociation. The structures in Figure 19.12 all show intimate contact between IF1 and helix H44 of the 16S rRNA in the 30S subunit. Helix H44 is also known to make extensive contact with the 50S ribosomal subunit. Ramakrishnan and coworkers speculated that the contact between IF1 and helix H44 perturbs the structure of helix H44 so as to resemble its structure in the transition state between association and dissociation of the ribosomal subunits. This would explain how IF1 accelerates both ribosomal association and dissociation.

SUMMARY The x-ray crystal structure of IF1 bound to the 30S ribosomal subunit shows that IF1 binds to the A site. In that position, it clearly blocks fMet-tRNA from binding to the A site, and may also actively promote fMet-tRNA binding to the P site through a presumed interaction between IF1 and IF2. IF1 also interacts intimately with helix H44 of the 30S subunit, and this may explain how IF1 accelerates both association and dissociation of the ribosomal subunits.

Fine Structure of the 50S Subunit

In 2000, Peter Moore and Thomas Steitz and their colleagues achieved a milestone in the study of ribosomal structure, and in the field of x-ray crystallography, by determining the crystal structure of a 50S ribosomal subunit at 2.4 Å resolution. They performed these studies on 50S subunits from the archaeon *Haloarcula marismortui,* because crystals of 50S subunits suitable for x-ray diffraction could be prepared from this organism. The structure, shown in Figure 19.13, includes 2833 of 3045 nucleotides in the rRNAs of the subunit (all 122 of the 5S rRNA nucleotides), and 27 of the subunit's proteins. The other proteins were not well ordered and could not be located accurately.

One clear difference between the two subunits lies in the tertiary structures of their rRNAs. Whereas the 16S rRNA in the 30S subunit assumed a three-domain structure, the 23S rRNA of the 50S subunit is a monolithic structure with no clear boundaries between domains. Moore, Steitz, and colleagues speculated that the reason for this difference is that the structural domains of the 30S subunit have to move relative to one another, whereas most of those in the 50S subunit do not.

The smaller structures in Figure 19.13 show the locations of the proteins in the 50S subunit. As we saw earlier in this chapter, the proteins in the 50S subunit are generally missing from the interface between the two subunits, particularly in the center, where the peptidyl transferase active site is thought to lie. This was a provocative finding because some uncertainty (Chapter 18) surrounded the question whether the peptidyl transferase activity lies in the RNA or protein of the 50S subunit.

To determine whether proteins are present at the peptidyl transferase active site, one needs to identify the active

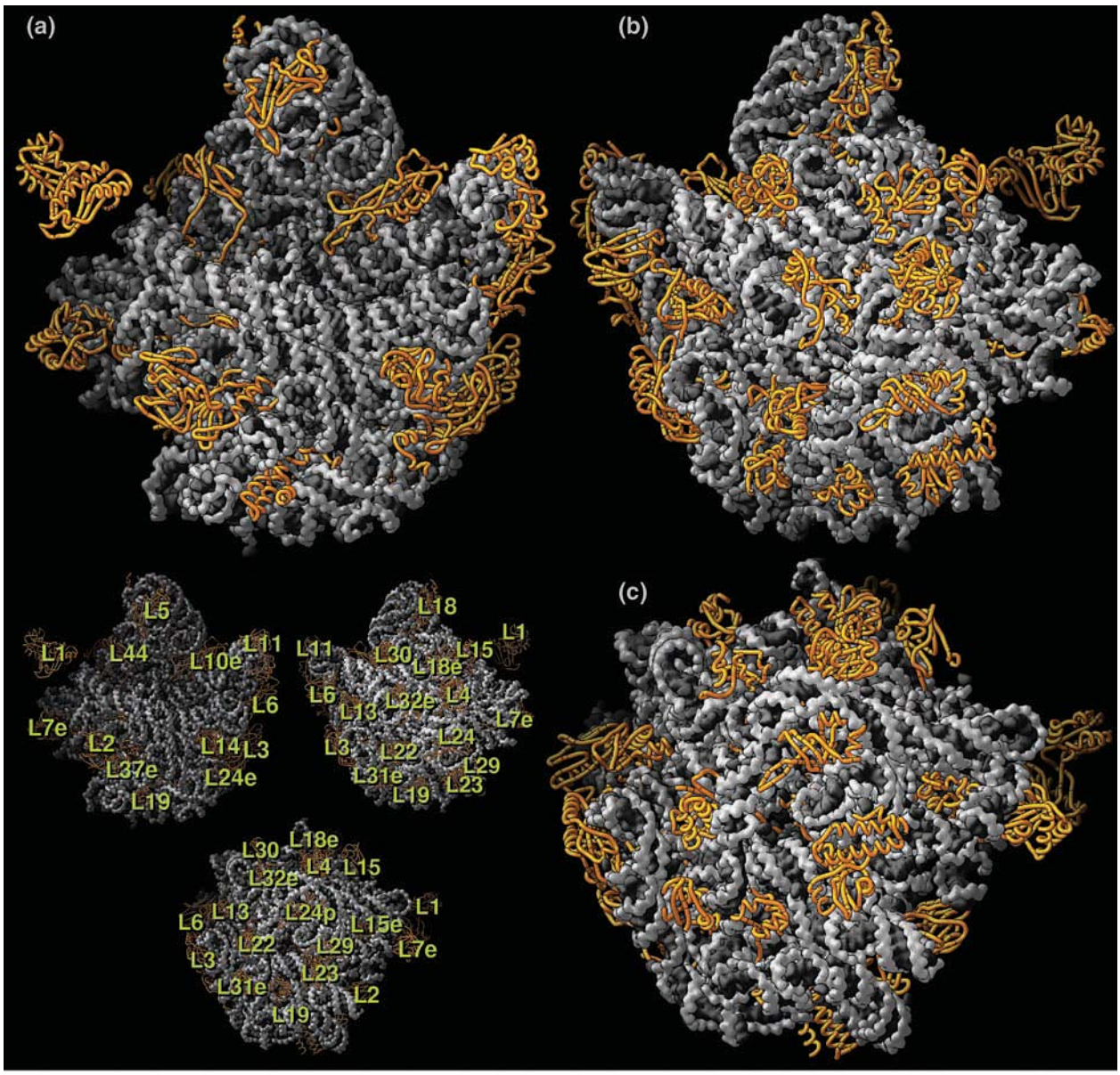

Figure 19.13 Crystal structure of the 50S ribosomal subunit from *Haloarcula marismortui.* The three large structures show the subunit in three different orientations: **(a)** front, or "crown" view (so named because of the resemblance to a three-pointed crown); **(b)** back view (crown view rotated 180 degrees); **(c)** bottom view, showing the end of the polypeptide exit tunnel at center. The RNA is gray and the proteins are gold. The three small structures at lower left are the same three orientations, with the proteins identified. The letter "e" after some numbers designates archaeal proteins that have only eukaryotic (not bacterial) homologs. (*Source:* Ban, N., P. Nissen, J. Hansen, P.B. Moore, and T.A. Steitz, The complete atomic structure of the large ribosomal subunit at 2.4 Å resolution. *Science* 289 (11 Aug 2000) f. 7, p. 917. Copyright © AAAS.)

site in a crystal structure. To accomplish this goal, Moore, Steitz, and coworkers soaked crystals of 50S subunits with two different peptidyl transferase substrate analogs, then performed x-ray crystallography and calculated electron difference maps. This located the electron densities corresponding to the substrate analogs, and therefore to the active site. One analog (CCdAp-puromycin) was designed by Michael Yarus to resemble the transition state, or intermediate, during the peptidyl transferase reaction. Thus, it is called the "Yarus analog."

Figure 19.14 shows that the Yarus analog lies in the cleft in the face of the 50S subunit, right where the active site was predicted to be. And no proteins are around, only RNA. The same behavior was observed for the other analog. Figure 19.15 is a model of the active site with all RNA removed, so we can see just how far the proteins are from the phosphate of the Yarus analog, which corresponds to the tetrahedral carbon atom at the very center of the transition state in the active site. The nearest protein is L3, which is more than 18 Å away from this

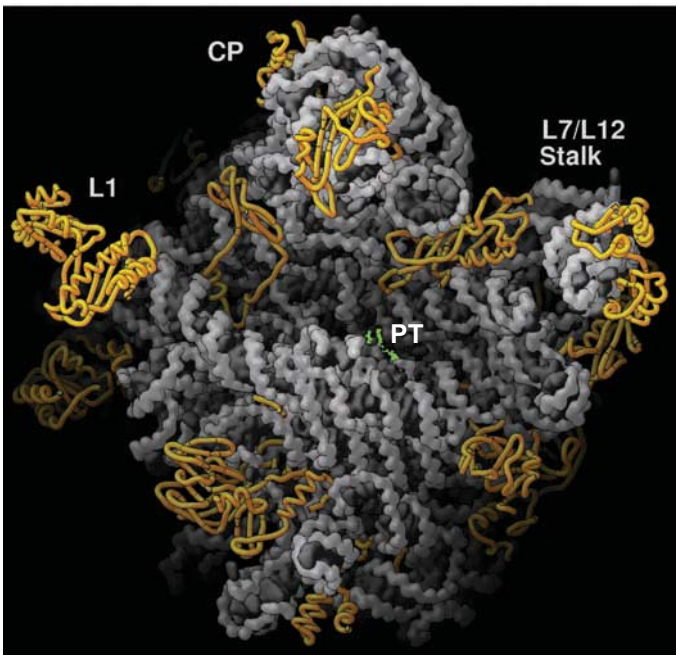

Figure 19.14 Location of the peptidyl transferase active site. This is a crown view of the 50S subunit as in Figure 19.13, with the location of the Yarus analog, which should be at the peptidyl transferase (PT) active site, in green. Notice the absence of proteins (gold) close to the active site. (*Source:* Ban, N., P. Nissen, J. Hansen, P.B. Moore, and T.A. Steitz, The complete atomic structure of the large ribosomal subunit at 2.4 Å resolution. *Science* 289 (11 Aug 2000) f. 2, p. 907. Copyright © AAAS.)

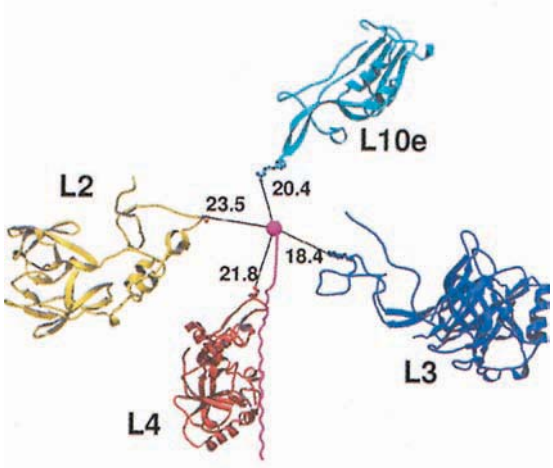

Figure 19.15 Peptidyl transferase active site with all RNA removed. The phosphate of the Yarus analog, at the center of the active site, is rendered in magenta (dark pink), with a long magenta tail representing a growing polypeptide. The four proteins closest to the active site are pictured, along with measurements of the closest approach (in Å) of each protein to the active site. (*Source:* Nissen, P., J. Hansen, N. Ban, P.B. Moore, and T.A. Steitz, The structural basis of ribosome activity in peptide bond synthesis. *Science* 289 (11 Aug 2000) f. 6b, p. 924. Copyright © AAAS.)

active site—much too far to play any direct role in catalysis.

If protein is absent from the active site, RNA must have the enzymatic activity. The crystal structure reveals that adenine 2486 (A2486), which corresponds to A2451 in *E. coli,* is closest to the tetrahedral carbon at the active center. This base is conserved in ribosomes from every species examined from all three kingdoms of life, which suggests it plays a crucial role. Furthermore, chloramphenicol and carbomycin, which inhibit peptidyl transferase, bind at or near A2451 in *E. coli.* And *E. coli* cells with mutations in A2451 are chloramphenicol-resistant, further implicating this base in the reaction.

If this model is correct, then mutations in A2486 would be expected to reduce peptidyl transferase activity by orders of magnitude. Alexander Mankin and colleagues tested this prediction in 2001 by reassembling a *T. aquaticus* 50S subunit from isolated proteins and 23S rRNAs with all three possible mutations in A2451, the base equivalent to A2486 in *H. marismortui,* then testing the reconstituted 50S subunits for peptidyl transferase activity by four different assays, including the fragment reaction described in Chapter 18. None of the mutations caused a dramatic decrease in activity; each mutated 23S rRNA could support at least 44% of wild-type activity in at least one of the assays.

If the adenine of A2486 does not play a major catalytic role in the peptidyl transferase reaction, what does? Scott Strobel and colleagues presented evidence in 2004 that implicates the 2′-hydroxyl group of the terminal adenosine of the peptidyl-tRNA in the P site. Figure 19.16 shows the position of this 2′-OH group with respect to the amino acid in the A site, which is making a nucleophilic attack on the carbonyl carbon that links the peptide to the tRNA in the P site. This attack will result in the joining of the peptide in the P site to the aminoacyl-tRNA in the A site, which is **transpeptidation,** the reaction catalyzed by peptidyl

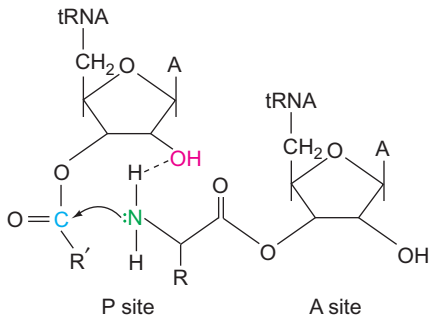

Figure 19.16 Positions of the tRNAs in the A and P sites during the peptidyl transferase reaction. The 2′-OH of the P site tRNA is in red; the amino nitrogen of the aminoacyl-tRNA in the A site is in green, and the carbonyl carbon of the peptidyl tRNA in the P site is in blue. Note the proximity of the 2′-OH of the P site tRNA to the attacking amino nitrogen in the A site.

transferase. It is clear that the 2′-OH group is very well positioned to play a role in this reaction by forming a hydrogen bond with one of the protons on the amino group, thus making the amino nitrogen a better nucleophile.

If this hypothesis is correct, removing the oxygen from the 2′-position of the terminal adenosine (A76) of the peptidyl-tRNA should impair the peptidyl transferase activity. Strobel and colleagues tested this idea in two ways: by replacing the 2′-hydroxyl group with a hydrogen atom (2′-deoxyadenosine, dA) or a fluorine atom (2′-deoxy, 2′-fluoroadenosine, fA). When they made either of these changes to the terminal adenosine of the tRNA in the P site, peptidyl transferase activity was severely inhibited.

To do their assay, Strobel and colleagues loaded [^{35}S] fMet-tRNA into the P site, then Lys-tRNA into the A site. This Lys-tRNA was added in separate experiments in three forms with respect to the terminal adenosine: normal, dA, and fA. Then they allowed peptidyl transferase and one round of translocation, placing [^{35}S]fMet-Lys-tRNA in the P site. This set the stage for adding puromycin and observing the rate of labeled peptidyl-puromycin release from the ribosome. Because puromycin binds very rapidly to the A site, peptidyl transferase is rate-limiting in peptidyl-puromycin release, so the release rate can be taken as a measure of the rate of peptidyl transferase. Strobel and colleagues separated the released labeled peptidyl-puromycin from other labeled substances using thin-layer electrophoresis, and determined the radioactivity in the product by phosphorimaging.

Figure 19.17 shows the results. With the normal tRNA substrate, the peptidyl transferase reaction was complete by the first time point (10 s). However, with either modified substrate, essentially no reaction occurred, even after 24 h. Thus, substituting either a hydrogen atom or a fluorine atom for the 2′-hydroxyl group of the tRNA in the P site completely blocked the peptidyl transferase reaction, strongly suggesting that this 2′-hydroxyl group is required for the reaction. The same behavior was observed with the three substrates and ordinary Phe-tRNA, rather than puromycin, in the A site, further supporting the importance of the 2′-hydroxyl group.

This study still left in question the role of the highly conserved A2451 (using the *E. coli* numbering) of the 23S rRNA. To probe that question, Norbert Polacek and colleagues devised a method to change the nature, not only of the base, but also of the sugar of A2451. When they removed the adenine base from A2451, creating an abasic site, little change occurred in peptidyl transferase activity, as measured by the familiar fMet-puromycin release assay. However, when they removed the 2′-hydroxyl group of A2451, they reduced activity almost 10-fold. Furthermore, when they removed the base as well as the 2′-OH group, they almost completely abolished activity. By contrast, performing the same changes in the adjoining nucleoside, A2450, had only modest effects on activity, emphasizing again the special importance of A2451.

The loss of activity in the ribosomes lacking the 2′-OH at position 2451 of the 23S rRNA could be due to lowered affinity for tRNA at the P site. If so, raising the concentration of fMet-tRNA should have enhanced activity, but it did not. So what is the role of this hydroxyl group? The evidence we just examined for the participation of the 2′-hydroxyl group

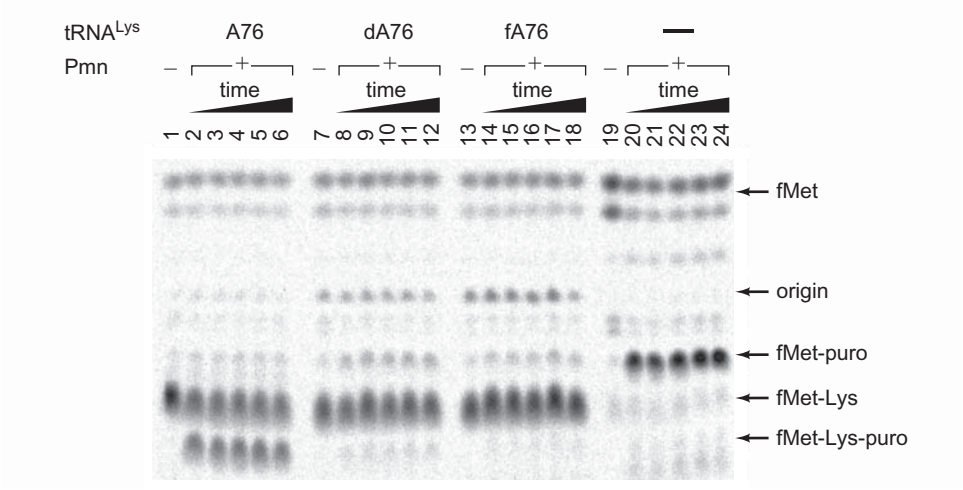

Figure 19.17 Peptidyl transferase activities with modified tRNAs. Strobel and colleagues carried out the peptidyl transferase reaction using a labeled dipeptidyl-tRNA in the P site and puromycin added to the A site. The tRNA in the P site contained a normal A76, dA76, or fA76, or simply fMet-tRNA with no modification (−), as indicated at top. They carried out the reactions for various times (10 s, 1 min, 6 min, 1 h, and 24 h in the presence of puromycin, or with no puromycin (−), also indicated at top. They separated labeled dipeptidyl-puromycin (fMet-Lys-puro) from other reactants and products by thin-layer electrophoresis, and subjected the electropherogram to phosphorimaging. Only the normal A76 in the P site tRNA was able to support measurable peptidyl transferase activity. (*Source:* Reprinted from *Nature Structural & Molecular Biology,* vol 11, Joshua S. Weinger, K. Mark Parnell, Silke Dorner, Rachel Green & Scott A. Strobel, "Substrate-assisted catalysis of peptide bond formation by the ribosome," Fig. 3a, p. 1103. Copyright 2004, reprinted by permission from Macmillan Publishers Ltd.)

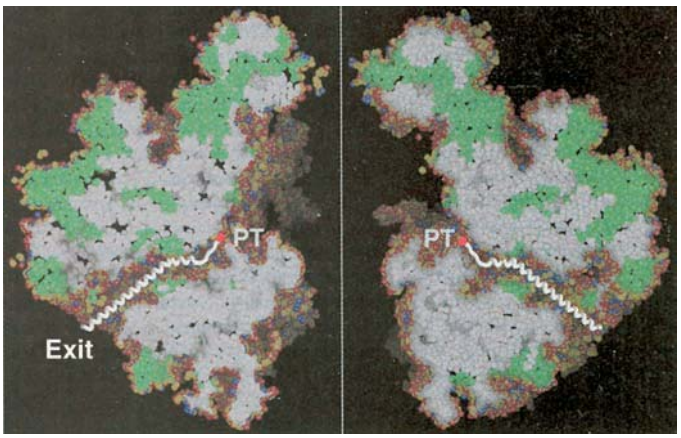

Figure 19.18 The polypeptide exit tunnel. The 50S subunit is pictured as if it were a fruit cut through the middle and opened up. This view reveals the exit channel leading away from the peptidyl transferase site (PT). A white α-helix is placed in the channel to represent an exiting polypeptide. (*Source:* Ban, N., P. Nissen, J. Hansen, P.B. Moore, and T.A. Steitz, The structural basis of ribosome activity in peptide bond synthesis. *Science* 289 (11 Aug 2000) f. 11a, p. 927. Copyright © AAAS.)

of the P site tRNA in the chemistry of transpeptidation is strong, but it remains possible that the 2′-hydroxyl group of A2451 also participates in this way. Alternatively, one or both of these hydroxyl groups could contribute to catalysis by helping to position the reactants properly in the active site. In contrast to the *Haloarcula* ribosome structure, a protein (the N-terminus of L27) in the *E. coli* ribosome is close enough to the peptidyl transferase center to be cross-linked to the 3′-end of the P site tRNA. However, given the strong evidence for RNA as the catalytic agent in one bacterium, it is unlikely that RNA does not play this role in another. Perhaps the N-terminus of L27 helps stabilize the peptidyl tRNA in the P site in the *E. coli* ribosome.

As the polypeptide product grows, it is thought to exit the ribosome through a tunnel in the 50S subunit. Moore, Steitz, and coworkers' studies also shed considerable light on this issue. Figure 19.18 shows a model of the 50S subunit cleaved in half to reveal the exit tunnel. The peptidyl transferase center has been marked, and a polypeptide modeled in the tunnel. The tunnel has an average diameter of 15 Å and narrows in two places to as little as 10 Å, just wide enough to accommodate a protein α-helix, so any further folding of the nascent polypeptide is unlikely. Much of the tunnel wall is made of hydrophilic RNA, so the exposed hydrophobic residues in a nascent polypeptide are not likely to find much in the tunnel wall to which to bind and retard the exit process.

SUMMARY The crystal structure of the 50S ribosomal subunit from *H. marismortui* has been determined to 2.4 Å resolution. This structure reveals relatively few proteins at the interface between ribosomal subunits, and no protein within 18 Å of the peptidyl transferase active center tagged with a transition state analog. The 2′-OH group of the tRNA in the P site is very well positioned to form a hydrogen bond to the amino group of the aminoacyl-tRNA in the A site, and therefore to help catalyze the peptidyl transferase reaction. In accord with this hypothesis, removal of this hydroxyl group eliminates almost all peptidyl transferase activity. Similarly, removal of the 2′-OH group of A2451 of the 23S rRNA strongly inhibits peptidyl transferase activity. This group may also participate in catalysis by hydrogen bonding, or it may help position the reactants properly for catalysis. The exit tunnel through the 50S subunit is just wide enough to allow a protein α-helix to pass through. Its walls are made of RNA, whose hydrophilicity is likely to allow exposed hydrophobic side chains of the nascent polypeptide to slide through easily.

Ribosome Structure and the Mechanism of Translation

As suggested in Chapter 18, the mechanism of translation presented there, including the three-site (A, P, E) model of the ribosome, was oversimplified. We have already seen that aminoacyl-tRNAs can exist in hybrid states that do not conform to the three-site model. The example we saw in Chapter 18 was the P/I state, which fMet-tRNA$_f^{Met}$ assumes without help from EF-P. But other hybrid states also exist. In this section we will examine structural studies that have shed considerably more light on the mechanism of translation.

Binding an Aminoacyl-tRNA to the A Site Single-particle cryo-electron microscopy (cryo-EM) studies as early as 1997 detected that an incoming aminoacyl-tRNA was first bent into the **A/T state**, in which the anticodon is interacting with the codon in the A site, but the amino acid and acceptor stem are still interacting with EF-Tu–GTP, rather than with the A site of the 50S subunit. Only upon GTP hydrolysis does the aminoacyl-tRNA unbend and fully enter the A site of the ribosome—a process known as **accommodation**.

In 2009, Ramakrishnan and colleagues used the higher-resolution x-ray crystallography method to clarify the details of the process by which EF-Tu brings a new aminoacyl-tRNA into the A site. They made crystals of the *T. thermophilus* ribosome complexed with mRNA, tRNA^{Phe} in the P and E sites, and the ternary complex of EF-Tu–Thr-tRNA^{Thr}–GDP. They also included the antibiotic kirromycin,

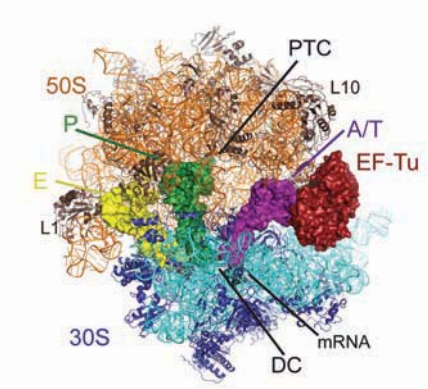

Figure 19.19 Crystal structure of the ribosome with deacylated tRNAs in the P and E sites and an aminoacyl-tRNA in the A/T state. EF-Tu and tRNAs are represented as surfaces, and the rRNA and proteins as cartoons. The 30S particle is depicted in cyan (RNA) and purple (proteins), and the 50S particle in orange (RNA) and brown (proteins). The tRNA in the E site is in yellow, the tRNA in the P site in green, and the aminoacyl-tRNA in the A/T state in magenta, bound to EF-Tu in red. DC, decoding center; PTC, peptidyl transferase center; L1, the L1 stalk of the 50S particle, which contains the L1 ribosomal protein. Note the empty A site in the 50S particle, into which the amino acid and acceptor stem of the aminoacyl-tRNA will move upon GTP hydrolysis. (*Source:* Reprinted with permission of *Science,* 30 October 2009, Vol. 326, no. 5953, pp. 688–694, Schmeing et al, The Crystal Structure of the Ribosome Bound to EF-Tu and Aminoacyl-tRNA. © 2009 AAAS.)

which prevents rearrangement of EF-Tu after GTP hydrolysis. The intent was to catch the aminoacyl-tRNA in the A/T state. Finally, they included paromomycin, which we have already learned stabilizes the binding between codon and anticodon.

As hoped, the aminoacyl-tRNA was in the A/T state, as shown in Figure 19.19. One can see that the +anticodon end of the aminoacyl-tRNA (magenta) is in the decoding center of the 30S ribosomal particle next to the mRNA, but the aminoacyl-tRNA is bent to the right by about 30° so its acceptor stem contacts EF-Tu, rather than inserting into the A site next to the peptidyl transferase center (PTC). Closer inspection showed that this bend is smooth and does not involve a kink in the tRNA.

What is the advantage of this tRNA bending? It requires energy, and this energy is provided by the correct interaction of a codon and its cognate anticodon. But binding a noncognate tRNA does not release as much energy, so the tRNA bend required to achieve the A/T state does not occur as readily. Thus, the requirement for the tRNA bend serves the purpose of translational fidelity by selecting against noncognate aminoacyl-tRNAs. This hypothesis is supported by the existence of several tRNA mutations that facilitate the bending required for the A/T state. These mutations result in lower translational fidelity because they make it easier to accommodate noncognate aminoacyl-tRNAs.

We know the bent aminoacyl-tRNA must straighten up to enter the A site, and this is relatively easy because the aminoacyl-tRNA makes contacts mostly with the decoding center and EF-Tu, with few contacts with the ribosome in between. The energy stored in the bent tRNA is more than enough to break these few contacts and cause the aminoacyl-tRNA to enter fully into the A site.

How does the ribosome collaborate with the GTPase of EF-Tu to cleave the GTP in the ternary complex, but only when a cognate aminoacyl-tRNA is in the decoding center? The GTPase center of EF-Tu is presumed to include elements called the P loop, switch I, and switch II. Switch II includes the putative catalytic residues Gly 83 and His 84. GTP cannot be hydrolyzed by the ternary complex itself because, in the absence of the ribosome, Gly 83 and His 84 are kept out of the GTPase active center by a hydrophobic gate composed of Ile 60 of switch I and Val 20 of the P loop. When this gate is opened, the catalytic residues can reach the catalytic center and activate a water molecule that hydrolyzes the GTP.

The present structure represents the post-GTP hydrolysis state, so we would expect the catalytic His 84 to be remote from the GDP, and it is. In addition, the P loop and switch II elements are well-ordered, but the region of switch I that contains the Ile 60 gate is not. This means that this part of switch I can move in the crystal structure, which gives rise to the hypothesis that this is the gate that swings open to allow the catalytic residues access to the GTP.

But what opens the gate? Figure 19.20 presents Ramakrishnan and colleagues' hypothesis, with the numbers in black circles representing the following events in order: (1) The process begins with the interaction of a codon and its cognate anticodon in the decoding center (16S rRNA residues A1492, A1493, and G530). (2) When the decoding center senses the proper fit between codon and anticodon, it causes the 30S subunit to undergo "domain closure," which shifts the 16S rRNA shoulder region into contact with EF-Tu. (3) This contact shifts the position of the β-turn of EF-Tu domain 2. (4) This shift in the β-turn changes the conformation of the acceptor stem of the aminoacyl-tRNA

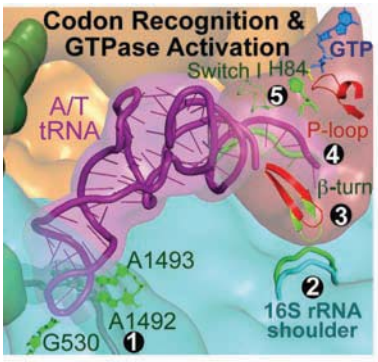

Figure 19.20 Codon recognition and GTPase activation. The aminoacyl-tRNA (magenta) is shown in the A/T state with its anticodon in the decoding center, and its accepter stem bound to EF-Tu. Only relevant parts of EF-Tu (β-turn [or loop], P-loop, switch I, and His 84 [H84]) are shown. The steps denoted by the white numbers in black circles are described in the text. (*Source:* Reprinted with permission of *Science,* 30 October 2009, Vol. 326, no. 5953, pp. 688–694, Schmeing et al, The Crystal Structure of the Ribosome Bound to EF-Tu and Aminoacyl-tRNA. © 2009 AAAS.)

to help bend the tRNA into the A/T state. (5) The change in conformation of the acceptor stem of the tRNA breaks its contacts with switch I, which allows the latter to move, opening the gate and allowing His 84 to move into the GTPase catalytic center and hydrolyze the GTP. One feature not illuminated by this study is the role of the L10–L12 stalk of the 50S particle, which is known to stimulate the GTPase activity of EF-Tu. The L10–L12 stalk was disordered in this crystal structure, and was therefore not seen.

The molecular interactions described in this section, including the bending of the aminoacyl-tRNA in the A/T state, the activation of the GTPase of EF-Tu, and the unbending of the aminoacyl-tRNA are shown in a movie (movie s1) at www.sciencemag.org/cgi/content/full/1179700/DC1. The three-dimensional effect of the movie shows these events much more clearly than a static, two-dimensional picture can. In addition, the movie shows what happens after GTP hydrolysis: EF-Tu–GDP leaves the A site, which allows the aminoacyl-tRNA to unbend into the full A/A state. This "accommodation" of the aminoacyl-tRNA by the A site causes a shift in the conformations of both the 30S and 50S ribosomal subunits. In particular, the mobile L1 stalk of the 50S particle moves, opening the E site and allowing the deacylated tRNA to leave the ribosome. Other studies had previously implicated the L1 stalk in release of the E site tRNA.

SUMMARY An aminoacyl-tRNA, upon binding to a ribosome, first enters the A/T state with its anticodon in the decoding site of the 30S particle, and its acceptor stem still bound to EF-Tu. This forces a bend in the tRNA, which occurs most readily with a perfect match between codon and anticodon, thus enhancing accuracy. Upon bending, the tRNA loses contact with switch I of EF-Tu, allowing switch I to move, which permits His 84 to enter the GTPase active center and hydrolyze GTP. Upon GTP hydrolysis, EF-Tu–GDP leaves the ribosome, allowing the aminoacyl-tRNA to enter the A/A state. This rearrangement in turn causes a conformational shift in the ribosome that releases the deacylated tRNA from the E site.

Translocation Danesh Moazed and Harry Noller used chemical footprinting studies in 1989 to show that, after peptidyl transfer but before translocation, the tRNAs in the A and P sites spontaneously shift their acceptor stems to the P and E sites, respectively, of the 50S subunit. This shift occurs even before EF-G binds to the ribosome and is driven by a ratcheting motion of the 30S and 50S subunits by 6° relative to each other. However, the anticodons remain paired with codons in the A and P sites, respectively, of the 30S subunit. Thus, these tRNAs have assumed hybrid A/P and P/E states. Only upon EF-G binding and EF-G-dependent hydrolysis of GTP do the anticodon stem-loops shift, along with the mRNA, in the 30S subunit to bring the tRNAs fully into the P and E sites. These events are shown in Figure 19.21, and in a movie at www.mrc-lmb.cam.ac.uk/ribo/homepage/movies/translation_bacterial.mov. The movie shows things much more clearly because of the three-dimensional effect, and the ability to show changes smoothly through time. Furthermore, it summarizes what we know about the structural basis of all phases of translation: initiation, elongation, and termination.

In 2009, Ramakrishnan and colleagues determined the crystal structure of the *T. thermophilus* ribosome complexed with mRNA, EFG-GDP, and the antibiotic fusidic acid, which allows translocation and GTP hydrolysis, but blocks EFG-GDP release from the ribosome. This structure was predicted to be in the post-translocation state, with the tRNAs in the classic P and E states, rather than in pre-translocation hybrid A/P and P/E states, and indeed that was what Ramakrishnan and colleagues found. Also, as predicted, EF-G interacts with the ribosome via its domain IV in much the same way that the EF-Tu—aminoacyl-tRNA—GTP complex does.

A novel feature of this crystal structure is that it stabilized the mobile L1 and L10–L12 stalks of the 50S particle so they could be visualized. In the present context, the shape and position of the L10–L12 stalk is particularly important because it is known to participate in the GTPase reaction catalyzed by EF-G. Indeed, this structure shows that the carboxyl terminal domain (CTD) of L12 contacts the G′ domain of EF-G. However, Ramakrishnan and colleagues noted that mutations that would disrupt this contact inhibit only the release of the inorganic phosphate byproduct of the GTPase reaction, not the reaction itself. This led them to speculate that the spatial relationship of L12 and EF-G is somewhat different at the time of GTP hydrolysis, and that it then converts to the shape they observed, which is important for phosphate release. It is also likely that L12 behaves in the same way with respect to the GTPase center of EF-Tu.

SUMMARY Translocation begins with a spontaneous ratcheting of the 30S particle with respect to the 50S particle, which brings the tRNAs into hybrid A/P and P/E states. Upon EF-G–GTP binding and hydrolysis of GTP, the tRNAs and mRNA translocate on the 30S particle to enter the classical P and E sites, and the ratchet has reset. Structural studies on a complex containing the 70S ribosome, EFG–GDP, mRNA and fusidic acid have revealed that EF-G binds to the ribosome in much the same way that EF-Tu–aminoacyl-tRNA–GDP does. These studies have also shown how the L10-L12 stalk may stimulate the GTPase of EF-G (and EF-Tu).

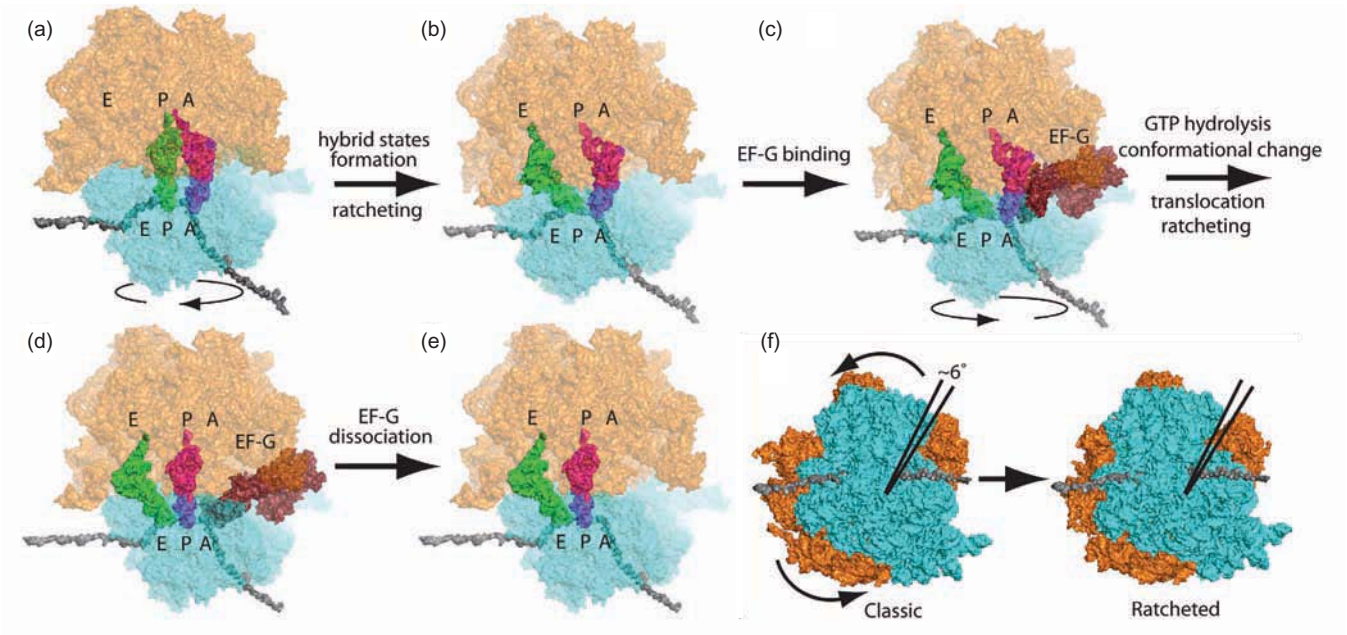

Figure 19.21 Structural basis of the translocation process. **(a)** The pretranslocation state with tRNAs in the classic A and P sites. The P site tRNA is deacylated. **(b)** Spontaneous ratcheting of the two subunits of the ribosome brings the two tRNAs into hybrid A/P and P/E states. **(c)** EF-G—GTP binds to the ribosome, with its domain IV closest to the A site. **(d)** GTP is hydrolyzed, which allows the mRNA and anticodon ends of the tRNAs to translocate on the 30S particle. This brings the two tRNAs into the classic P and E sites, and also allows relaxation of the ratchet back to its initial, pretranslocation state. **(e)** EF-G—GTP dissociates from the ribosome. **(f)** The ratchet. The 30S particle (cyan) rotates about 6° counter-clockwise relative to the 50S particle (brown) in going from the classic (left) to ratcheted (right) state. (*Source:* Reprinted by permission from Macmillan Publishers Ltd: *Nature* 461, 1234–1242 (29 October 2009) Schmeing & Ramakrishnan, What recent ribosome structures have revealed about the mechanism of translation. © 2009.)

Interaction of the 70S Ribosome with RF1 and RF2

Several structural studies have shown that the release factors, both prokaryotic and eukaryotic, resemble tRNAs and that certain amino acids at one end of the release factor molecule may act like an anticodon in interacting with the stop codon. In particular, a string of three amino acids in RF1 (PXT, where P is proline, T is threonine, and X is any amino acid) was predicted to recognize two stop codons, UAA and UAG. In 2008, Harry Noller and colleagues shed more light on this and other issues when they presented the x-ray crystal structure of a complex containing the *T. thermophilus* 70S ribosome, RF1, tRNA, and an mRNA that included a UAA stop codon.

Figure 19.22a and b compare the positions of RF1 and an aminoacyl-tRNA in the A site of the ribosome. These panels, as well as the details shown in panels c and d, make it clear that parts of RF1, including domains 2 and 3, occupy essentially the same position in the A site that an aminoacyl-tRNA would normally fill. In particular, panels c and d suggest that a part of domain 2 (yellow), including the PXT motif (in this case, PVT, red), constitute a kind of "reading head" that closely approaches the stop codon in the mRNA and has the potential to make specific contacts to "read" the stop codon. Panels c and d also show that the other end of RF1 in the A site, the tip of domain 3 (purple), including the universally conserved GGQ motif (red) closely approaches the peptidyl transferase center (PTC) and therefore is in position to participate in the conversion of the peptidyl transferase activity to an esterase activity that cleaves the polypeptide from the tRNA, terminating translation. Below, we will examine the role of the codon recognition end (the reading head) of RF1 in more detail.

Figure 19.23 depicts the codon recognition site of the complex, and demonstrates that the previously suggested simple recognition of UAA by the PXT motif was far too simple. The PXT motif does indeed play an important role, but it discriminates the first two bases of the UAA codon, rather than the last two, as previously proposed, and it is aided by other conserved parts of RF1 and the 16S rRNA. Specifically, Figure 19.23b shows that T186 of the PXT motif helps to recognize U1 and A2 of the UAA codon by forming hydrogen bonds with both bases. In addition, the protein backbone at glycine 116 and glutamate 119 makes two hydrogen bonds with U1 of the UAA codon. Also, A2 of the stop codon stacks between stop codon base A1 and histidine 193 of RF1. Finally, the 2′-hydroxyl groups of the ribose moieties of U1 and A2 make hydrogen bonds to phosphate 1493 and the ribose of A1492, respectively, of the 16S rRNA (using the *E. coli* numbering system). All of these interactions work best with the U and A in the first two positions of the stop codon. It is interesting that A1492 and A1493 participate in binding normal codons (see earlier in this chapter) and the stop codon, but their roles are much different with the two types of codon.

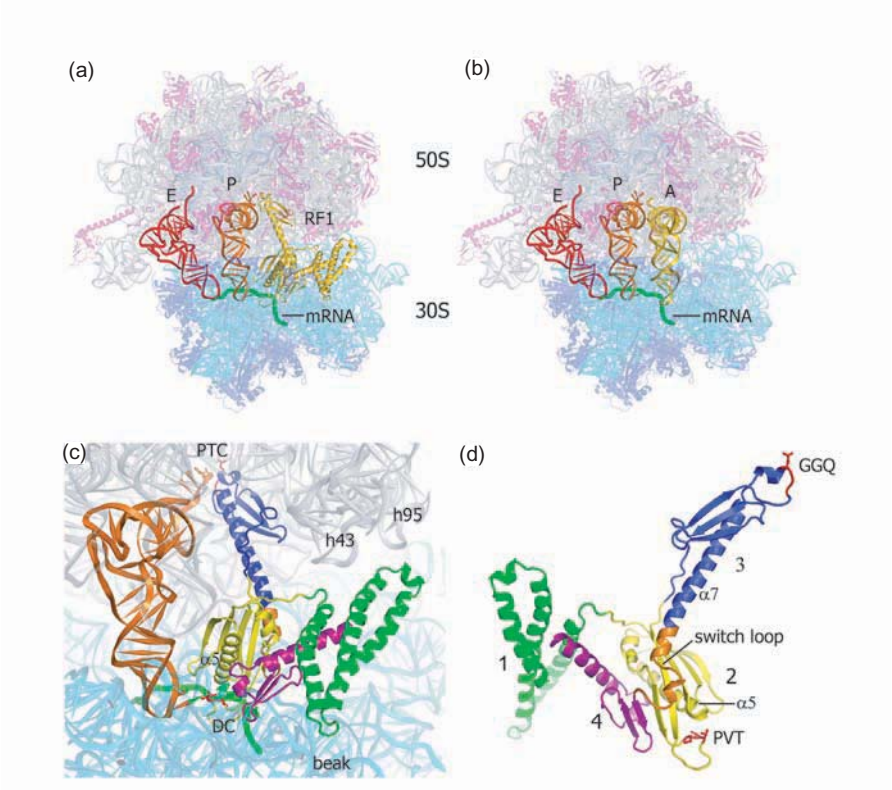

Figure 19.22 Structure of the RF1-ribosome complex. (a) Positions of RF1, P site tRNA, E site tRNA, and mRNA in the 70S-ribosome. **(b)** Positions of A site tRNA, P site tRNA, E site tRNA, and mRNA in the 70S ribosome. **(c)** Detail of the positions of RF1 and P site tRNA (orange) in the ribosome. PTC, peptidyltransferase center; DC, decoding center; h43 and h95, helices of 23S rRNA. **(d)** RF1 rotated 180° relative to panel (c). The domains of RF1 are denoted by the same colors as in panel (c): domain 1, green; domain 2, yellow; domain 3, purple; domain 4, magenta; PVT and GGQ motifs, red; switch loop, orange. (*Source:* Reprinted by permission from Macmillan Publishers Ltd: *Nature,* 454, 852–857, 14 August 2008. Laurberg et al, Structural basis for translation termination on the 70S ribosome. © 2008.)

An amino acid-encoding codon has all three bases stacked together, so they can base-pair with the three stacked bases of the corresponding anticodon. However, the crystal structure in Figure 19.23a and c shows that the third base (A3) of the stop codon UAA is widely separated from the others. This separation is caused by several factors. For one thing, His193 of RF1 inserts roughly where the third base of a normal codon would be, and stacks with A2. This pushes A3 away from A2 (to the right in Figure 19.20a), where it can interact with the following residues of IF1: Thr 194, Q 181, and the backbone carbonyl of I 192. In addition, G530 of the 16S rRNA stacks with A3, helping to stabilize its separation from A2.

Later in 2008, Ramakrishnan and colleagues published the crystal structure of RF2 bound to the *T. thermophilus* ribosome, including the UGA stop codon, which is specific for RF2. This structure confirmed that the anticodon-like tripeptide corresponding to PXT in RF1, which is (SPF; Ser-Pro-Phe) in RF2, acts like PTX in RF1 by closely approaching the decoding center, where it helps recognize the stop codon. In addition, just as the PXT motif in RF1 gets help from other residues in RF1 and 16S rRNA, the SPF motif in RF2 is important, but by no means acts alone in recognizing the UGA stop codon.

Ramakrishnan and colleagues also showed that the invariant GGQ motif in RF2, just like the same motif in RF1, is positioned very close to the peptidyl transferase center, where it presumably takes part in release of the polypeptide from the tRNA. Their structure showed that the two glycines in the motif assume conformations that would be impossible for any other amino acid, which explains why these two amino acids are universally conserved. The conformation of the GGQ places the Q in position to participate in the hydrolysis of the ester bond linking the polypeptide to the tRNA. This is also the way RF1 presumably works, which explains why the glutamine in the motif is universally conserved.

SUMMARY RF1 Domains 2 and 3 fill the codon recognition site and the peptidyl transferase site, respectively, of the ribosome's A site, in recognizing the UAA stop codon. The "reading head" portion of domain 2 of RF1, including its conserved PXT motif, occupies the decoding center within the A site and collaborates with A1493 and A1492 of the 16S rRNA to recognize the stop codon. The universally conserved GGQ motif at the tip of domain 3 of RF1 closely approaches the peptidyl transferase center and participates in cleavage of the ester

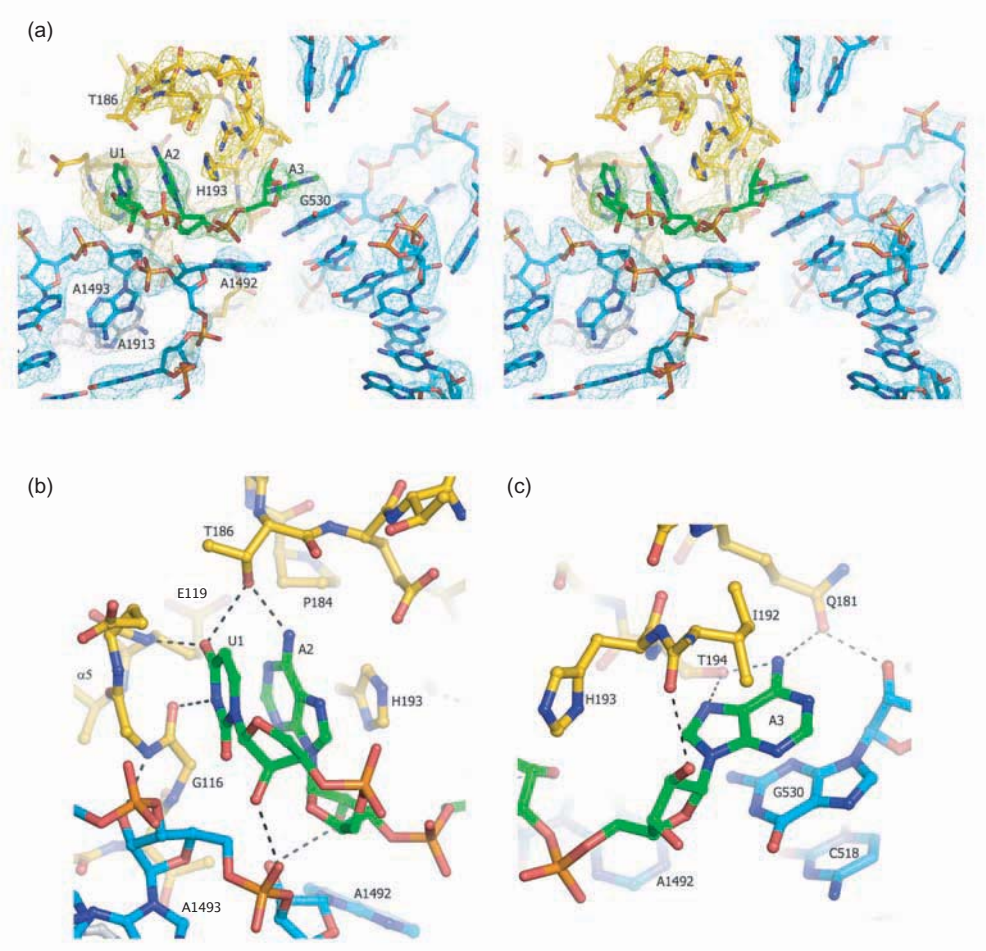

Figure 19.23 Detail of interactions between UAA stop codon and the decoding center. (a) Stereo diagram of the stop codon (green), the RFI reading head (yellow), 16S rRNA (cyan), and one base of 23S rRNA (A1913, gray). U1, A2, and A3 of the stop codon are labeled, as are key amino acids of RFI, and key bases of 16S rRNA. **(b** and **c)** Detail of interactions between the first two bases **(b)** and the last base **(c)** of the stop codon and the decoding center. Hydrogen bonds between key parts of the RFI protein and the 16S rRNA are shown as dashed lines. (*Source:* Reprinted by permission from Macmillan Publishers Ltd: *Nature,* 454, 852–857, 14 August 2008. Laurberg et al, Structural basis for translation termination on the 70S ribosome. © 2008.)

bond linking the completed polypeptide to the tRNA. RF2 binds to the ribosome in much the same way in response to the UGA stop codon. Its SPF motif, which corresponds to the PXT motif in RF1, is in position to recognize the stop codon, in collaboration with other residues in RF2 and the 16S rRNA. Its GGQ motif is at the peptidyl transferase center, where it can participate in cleavage of the polypeptide–tRNA bond, which terminates translation.

Polysomes

We have seen in previous chapters that more than one RNA polymerase can transcribe a gene at a time. The same is true of ribosomes and mRNA. In fact, it is common for many ribosomes to be traversing the same mRNA in tandem at any given time. The result is a polyribosome, or **polysome,** such as the one pictured in Figure 19.24. In this polysome we can count 74 ribosomes translating the mRNA simultaneously. We can also tell which end of the polysome is which by looking at the nascent polypeptide chains. These grow longer as the ribosome moves from the 5′-end (where translation begins) to the 3′-end (where translation ends). Therefore, the 5′-end is at lower left, and the 3′-end is at lower right.

Consider the process of forming a eukaryotic polysome. The first ribosome to load onto the mRNA faces the most difficult task in its "pioneer round" of translation. The mRNA comes from the nucleus loaded with proteins: Some of these are left over from the processes of splicing and polyadenylation; other mRNA-bound proteins help guide the mRNA out of the nucleus and protect it from destruction. But there is barely room for the mRNA itself between

the two ribosomal subunits, so these proteins must be stripped off as the mRNA threads through the first ribosome. These proteins are soon replaced by others that are required for the translation process.

Figure 19.24 Electron micrograph of a polysome from the midge *Chironomus.* The 5′-end on the mRNA is at lower left, and the mRNA bends up and then down to the 3′-end at lower right. The dark blobs attached to the mRNA are ribosomes. The fact that many (about 74) of them are present is the reason for the name *polysome.* Nascent polypeptides extend away from each ribosome and grow longer as the ribosomes approach the end of the mRNA. The faint blobs on the nascent polypeptides are not individual amino acids but domains containing groups of amino acids. (*Source:* Francke et al., Electron microscopic visualization of a discreet class of giant translation units in salivary glands of *Chironomus tetans. EMBO Journal* 1, 1982, pp. 59–62. European Molecular Biology Organization.)

The polysome in Figure 19.24 is from a eukaryote (a midge, or gnat). Because transcription and translation occur in different compartments in eukaryotes, polysomes will always occur in the cytoplasm, independent of the genes. Prokaryotes also have polysomes, but the picture in these organisms is complicated by the fact that transcription and translation of a given gene and its mRNA occur simultaneously and in the same location. Thus, we can see nascent mRNAs being synthesized and being translated by ribosomes at the same time. Figure 19.25 shows just such a situation in *E. coli.* We can see two segments of the bacterial chromosome running parallel from left to right. Only the segment on top is being transcribed. We can tell that transcription is occurring from left to right in this picture because the polysomes are getting longer as they move in that direction; as they get longer, they have room for more and more ribosomes. Do not be misled by the difference in scale between Figures 19.24 and 19.25; the ribosomes appear smaller, and the nascent protein chains are not visible in the latter picture. Remember also that the strands running across Figure 19.25 are DNA, whereas that in Figure 19.24 is mRNA. The mRNAs are more or less vertical in Figure 19.25.

SUMMARY Most mRNAs are translated by more than one ribosome at a time; the result, a structure in which many ribosomes translate an mRNA in tandem, is called a polysome. In eukaryotes, polysomes are found in the cytoplasm. In prokaryotes, transcription of a gene and translation of the resulting mRNA occur simultaneously. Therefore, many polysomes are found associated with an active gene.

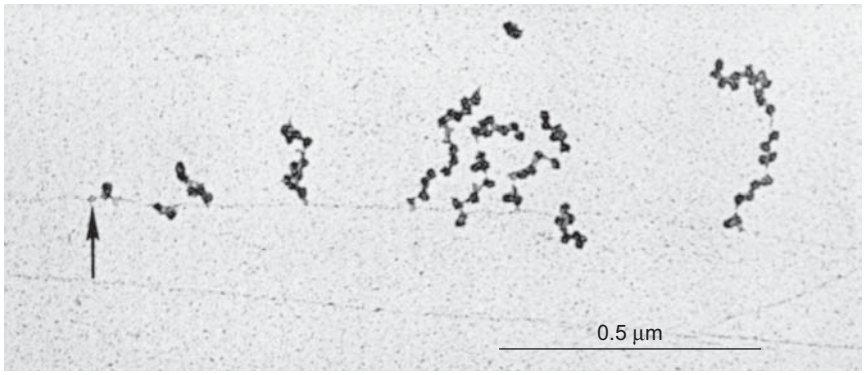

Figure 19.25 Simultaneous transcription and translation in *E. coli.* Two DNA segments stretch horizontally across the picture. The top segment is being transcribed from left to right. As the mRNAs grow, more and more ribosomes attach and carry out translation. This gives rise to polysomes, which are arrayed more or less perpendicular to the DNA. The nascent polypeptides are not visible in this picture. The arrow at left points to a faint spot, which may be an RNA polymerase just starting to transcribe the gene. Other such spots denoting RNA polymerase appear at the bases of some of the polysomes, where the mRNAs join the DNA. (*Source:* O.L. Miller, B.A. Hamkalo, and C.A. Thomas Jr., Visualization of bacterial genes in action. *Science* 169 (July 1970) p. 394. Copyright © AAAS.)

19.2 Transfer RNA

In 1958, Francis Crick postulated the existence of an adaptor molecule, presumably RNA, that could serve as a mediator between the string of nucleotides in DNA (actually in mRNA) and the string of amino acids in the corresponding protein. Crick favored the idea that the adapter contained two or three nucleotides that could pair with nucleotides in codons, although no one knew the nature of codons, or even of the existence of mRNA, at that time. Transfer RNA had already been discovered by Paul Zamecnik and coworkers a year earlier, although they did not realize that it played an adapter role.

The Discovery of tRNA

By 1957, Zamecnik and colleagues had worked out a cell-free protein synthesis system from the rat. One of the components of the system was a so-called pH 5 enzyme fraction that contained the soluble factors that worked with ribosomes to direct translation of added mRNAs. Most of the components in the pH 5 enzyme fraction were proteins, but Zamecnik's group discovered that this mixture also included a small RNA. Of even more interest was their finding that this RNA could be coupled to amino acids. To demonstrate this, they mixed the RNA with the pH 5 enzymes, ATP, and [^{14}C]leucine. Figure 19.26a shows that the more labeled leucine these workers added to the mixture, the more was attached to the RNA, which they separated from protein by phenol extraction. Furthermore, when they left out ATP, no reaction occurred. We now know that this reaction was the charging of tRNA with an amino acid.

Not only did Zamecnik and his coworkers show that the small RNA could be charged with an amino acid, they also demonstrated that it could pass its amino acid to a growing protein. They performed this experiment by mixing the [^{14}C]leucine-charged pH 5 RNA with microsomes—small sections of endoplasmic reticulum containing ribosomes. Figure 19.26b shows a near-perfect correspondence between the loss of radioactive leucine from the pH 5 RNA and gain of the leucine by the protein in the microsomes. This represented the incorporation of leucine from leucyl-tRNA into nascent polypeptides on ribosomes.

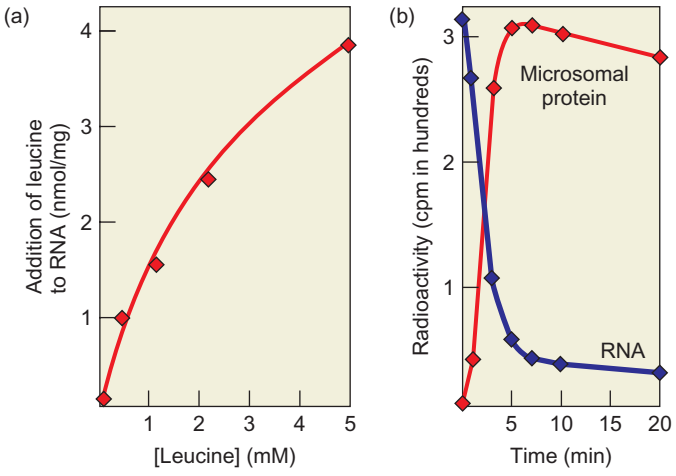

Figure 19.26 Discovery of tRNA. (a) tRNAs can be charged with leucine. Zamecnik and colleagues added labeled leucine to the tRNA-containing fraction and plotted the binding of leucine to the RNA as a function of labeled leucine added. **(b)** The charged tRNA can donate its amino acid to nascent protein. Zamecnik and colleagues followed the radioactivity (cpm) lost from the RNA (blue) and gained by the nascent proteins (red) in the microsomes, which contained the ribosomes. The reciprocal relationship between these curves suggested that the RNA was donating its amino acid to the growing protein. (*Source:* Adapted from Hoagland, M. B., et al., *Journal of Biological Chemistry* 231:244 & 252, 1958.)

SUMMARY Transfer RNA was discovered as a small RNA species independent of ribosomes that could be charged with an amino acid and could then pass the amino acid to a growing polypeptide.

tRNA Structure

To understand how a tRNA carries out its functions, we need to know the structure of the molecule, and tRNAs have a surprisingly complex structure considering their small size. Just as a protein has primary, secondary, and tertiary structure, so does a tRNA. The primary structure is the linear sequence of bases in the RNA; the secondary structure is the way different regions of the tRNA base-pair with each other to form stem-loops; and the tertiary structure is the overall three-dimensional shape of the molecule. In this section, we will survey tRNA structure and its relationship to tRNA function.

In 1965, Robert Holley and his colleagues completed the first determination ever of the base sequence of a natural nucleic acid, an alanine tRNA from yeast. This primary sequence suggested at least three attractive secondary structures, including one that had a cloverleaf shape. By 1969, 14 tRNA sequences had been determined, and it became clear that, despite considerable differences in primary structure, all could assume essentially the same "cloverleaf" secondary structure, as illustrated in Figure 19.27a. As we study this structure we should bear in mind that the real three-dimensional structure of a tRNA is not cloverleaf-shaped at all; the cloverleaf merely describes the base-pairing pattern in the molecule.

The cloverleaf has four base-paired stems that define the four major regions of the molecule (Figure 19.27b). The first, seen at the top of the diagram, is the **acceptor stem,** which includes the two ends of the tRNA, which are base-paired to each other. The 3′-end, bearing the invariant sequence CCA, protrudes beyond the 5′-end. On the left is

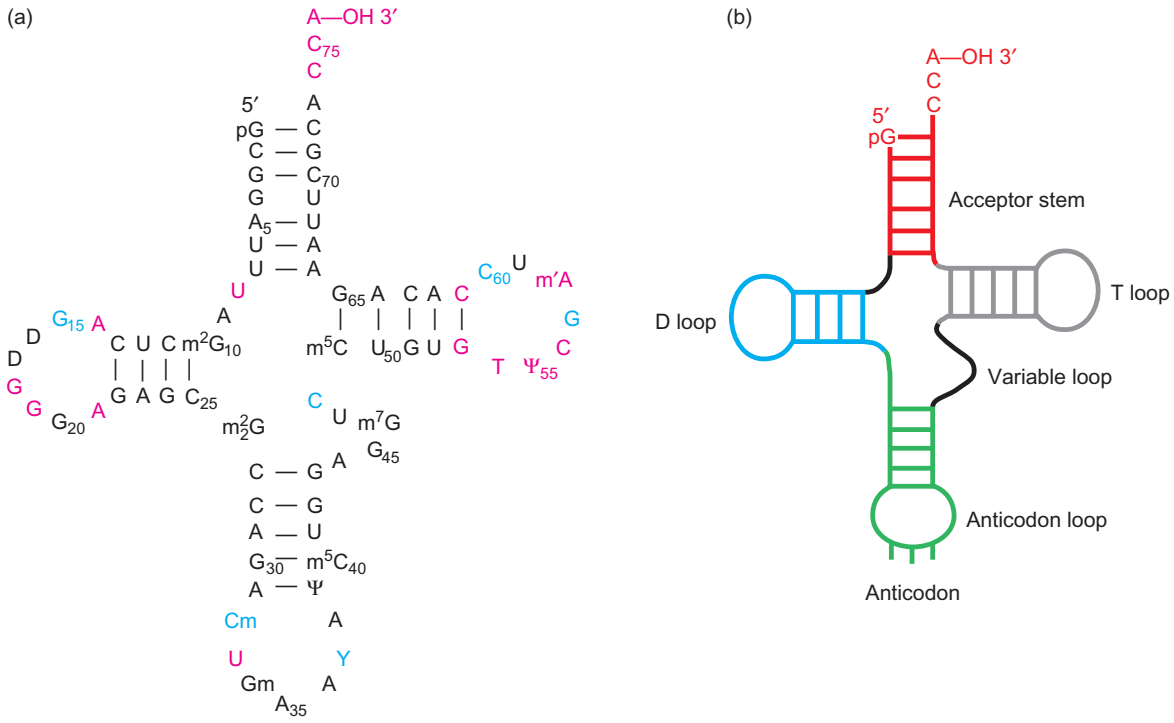

Figure 19.27 Two views of the cloverleaf structure of tRNA. **(a)** Base sequence of yeast $tRNA^{Phe}$, shown in cloverleaf form. Invariant nucleotides are in red. Bases that are always purines or always pyrimidines are in blue. **(b)** Cloverleaf structure of yeast $tRNA^{Phe}$. At top is the acceptor stem (red), where the amino acid binds to the 3′-terminal adenosine. At left is the dihydro U loop (D loop, blue), which contains at least one dihydrouracil base. At bottom is the anticodon loop (green), containing the anticodon. The T loop (right, gray) contains the virtually invariant sequence TΨC. Each loop is defined by a base-paired stem of the same color. (*Source:* (*a*) Adapted from Kim, S.H., F.L. Suddath, G.J. Quigley, A. McPherson, J.L. Sussman, A.H.J. Wang, N.C. Seeman, and A. Rich, Three-dimensional tertiary structure of yeast phenylalanine transfer RNA, *Science* 185:435, 1974.)

the **dihydrouracil loop** (**D loop**), named for the modified uracil bases this region always contains. At the bottom is the **anticodon loop,** named for the all-important anticodon at its apex. As we learned in Chapter 3, the anticodon base-pairs with an mRNA codon and therefore allows decoding of the mRNA. At right is the T loop, which takes its name from a nearly invariant sequence of three bases: TΨC. The Ψ stands for a modified nucleoside in tRNA, **pseudouridine.** It is the same as normal uridine, except that the base is linked to the ribose through the 5-carbon of the base instead of the 1-nitrogen. The region between the anticodon loop and the T loop in Figure 19.27 is called the **variable loop** because it varies in length from 4 to 13 nt; some of the longer variable loops contain base-paired stems.

Transfer RNAs contain many modified nucleosides in addition to dihydrouridine and pseudouridine. Some of the modifications are simple methylations. Others are more elaborate, such as the conversion of guanosine to a nucleoside called **wyosine,** which contains a complex three-ring base called the Y base (Figure 19.28). Some tRNA modifications are general. For example, virtually all tRNAs have a pseudouridine in the same position in the T loop, and most tRNAs have a hypermodified nucleoside such as wyosine next to the anticodon. Other modifications are specific for certain tRNAs. Figure 19.28 illustrates some of the common modified nucleosides in tRNAs.

The modification of tRNA nucleosides raises the question: Are tRNAs made with modified bases, or are the bases modified after transcription is complete? The answer is that tRNAs are made in the same way that other RNAs are made, with the four standard bases. Then, once transcription is complete, multiple enzyme systems modify the bases. What effects, if any, do these modifications have on tRNA function? At least two tRNAs have been made in vitro with the four normal, unmodified bases, and they were unable to bind amino acids. Thus, at least in these cases, totally unmodified tRNAs were nonfunctional. Although these studies suggested that the sum of all the modifications is critical, each individual base modification probably has more subtle effects on the efficiency of charging and tRNA usage.

In the 1970s, Alexander Rich and his colleagues used x-ray diffraction techniques to reveal the tertiary structure of tRNAs. Because all tRNAs have essentially the same secondary structure, represented by the cloverleaf model, it is perhaps not too surprising that they all have essentially the same tertiary structure as well. Figure 19.29 illustrates this inverted L-shaped structure for yeast $tRNA^{Phe}$. Perhaps the most important aspect of this structure is that it

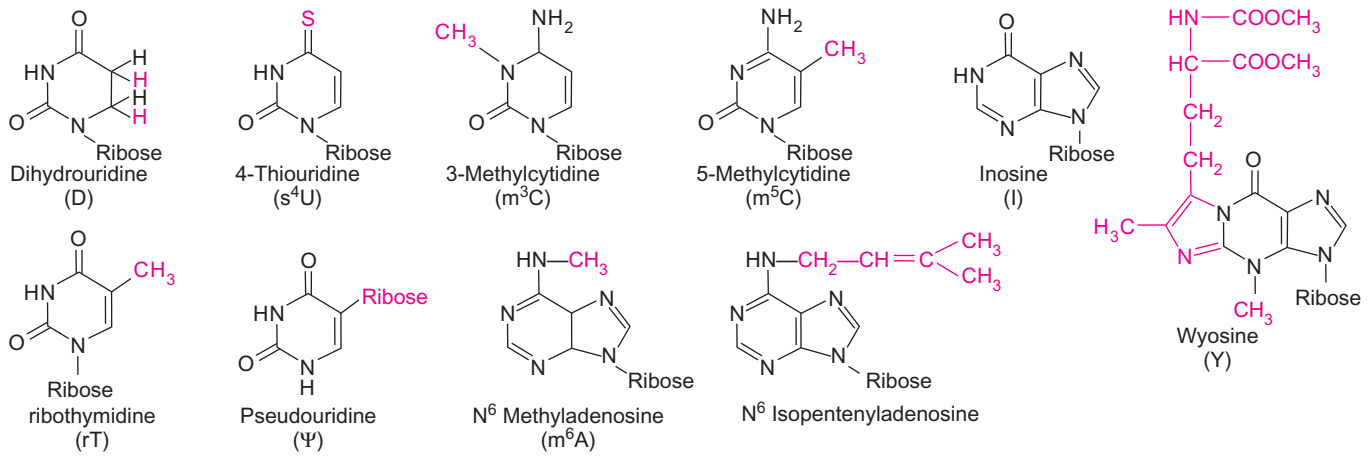

Figure 19.28 Some modified nucleosides in tRNA. Red indicates the variation from one of the four normal RNA nucleosides. Inosine is a special case; it is a normal precursor to both adenosine and guanosine.

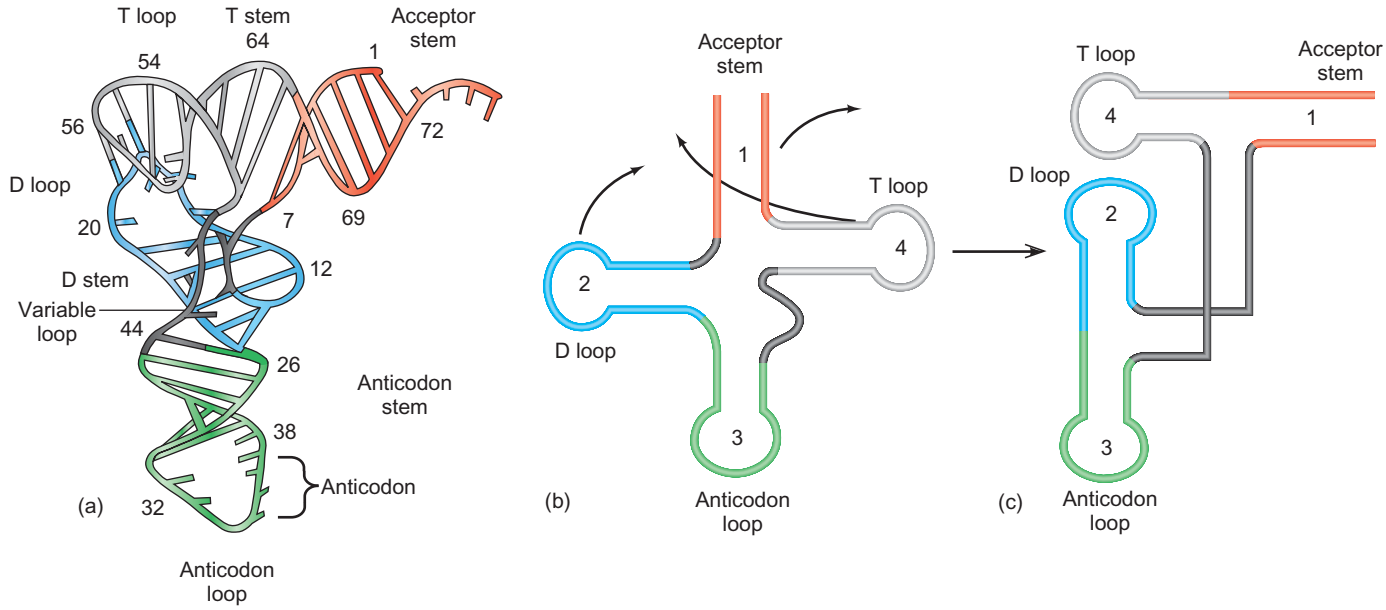

Figure 19.29 Three-dimensional structure of tRNA. (a) A planar projection of the three-dimensional structure of yeast $tRNA^{Phe}$. The various parts of the molecule are color-coded to correspond to (b) and (c). **(b)** Familiar cloverleaf structure of tRNA with same color scheme as part (a). Arrows indicate the contortions this cloverleaf would have to go through to achieve the approximate shape of a real tRNA, shown in part **(c).** (*Source:* Adapted from Quigley, G.J. and A. Rich, Structural domains of transfer RNA molecules, *Science* 194:197, Fig. 1b, 1976.)

maximizes the lengths of its base-paired stems by stacking them in sets of two to form relatively long extended base-paired regions. One of these regions lies horizontally at the top of the molecule and encompasses the acceptor stem and the T stem; the other forms the vertical axis of the molecule and includes the D stem and the anticodon stem. Even though the two parts of each stem are not aligned perfectly and the stems therefore bend slightly, the alignment allows the base pairs to stack on each other, and therefore confers stability. The base-paired stems of the molecule are RNA–RNA double helices. As we learned in Chapter 2, such RNA helices should assume an A-helix form with about 11 bp per helical turn, and the x-ray diffraction studies verified this prediction.

Figure 19.30 is a stereo diagram of the yeast $tRNA^{Phe}$ molecule. The base-paired regions are particularly easy to see in three dimensions, but you can even visualize them in two dimensions in the T stem-acceptor region because they are depicted almost perpendicular to the plane of the page, so they appear as almost parallel lines.

As we have seen, a tRNA is stabilized primarily by the secondary interactions that form the base-paired regions,

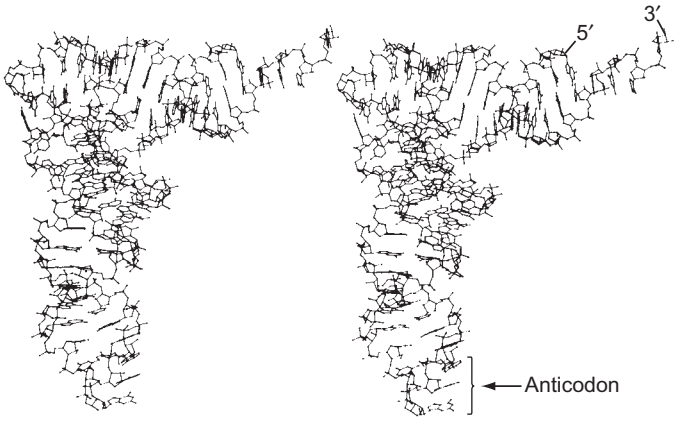

Figure 19.30 Stereo view of tRNA. To see the molecule in three dimensions, use a stereo viewer, or force the two images to merge either by relaxing your eyes as if focusing on something in the distance (the "magic eye" technique) or by crossing your eyes slightly. It may take a little time for the three-dimensional effect to develop. (*Source:* From Quigley, G.J. and A. Rich, Structural domains of transfer RNA molecules. *Science* 194 (19 Nov 1976) f. 2, p. 798. Copyright © AAAS. Reprinted with permission from AAAS.)

but it is also stabilized by dozens of tertiary interactions between regions. These include base–base, base–backbone, and backbone–backbone interactions. Most of the base–base tertiary interactions that involve hydrogen bonds occur between invariant or semi-invariant bases (the semi-invariant bases are always purines or always pyrimidines). Because these interactions allow the tRNA to fold into the proper shape, it makes sense that the bases involved tend not to vary; any variance would hinder the proper folding and hence the proper functioning of the tRNA. Only one of the base–base interactions is a normal Watson–Crick base pair (G19–C56). All the others are extraordinary. The G15–C48 pair, for example, which joins the D loop to the variable loop, cannot be a Watson–Crick base pair because the two strands are parallel here, rather than antiparallel. We call this a *trans*-pair. Several examples also occur of one base interacting with two other bases. One of these involves U8, A14, and A21. Now that the tertiary interactions have been discussed, you can look again at Figure 19.29a and see them in a more realistic form. Note for example the interactions between bases 18 and 55, and between bases 19 and 56. At first glance, these look like base pairs within the T loop; on closer inspection we can now see that they link the T loop and the D loop.

One other striking aspect of tRNA tertiary structure is the structure of the anticodon. Figure 19.30 demonstrates that the anticodon bases are stacked, but this stacking occurs with the bases projecting out to the right, away from the backbone of the tRNA. This places them in position to interact with the bases of the codon in an mRNA. In fact, the anticodon backbone is already twisted into a partial helix shape, which presumably facilitates base-pairing with the corresponding codon (recall Figure 19.2)

SUMMARY All tRNAs share a common secondary structure represented by a cloverleaf. They have four base-paired stems defining three stem-loops (the D loop, anticodon loop, and T loop) and the acceptor stem, to which amino acids are added in the charging step. The tRNAs also share a common three-dimensional shape, which resembles an inverted L. This shape maximizes stability by lining up the base pairs in the D stem with those in the anticodon stem, and the base pairs in the T stem with those in the acceptor stem. The anticodon of the tRNA protrudes from the side of the anticodon loop and is twisted into a shape that readily base-pairs with the corresponding codon in mRNA.

Recognition of tRNAs by Aminoacyl-tRNA Synthetase: The Second Genetic Code

In 1962, Fritz Lipmann, Seymour Benzer, Günter von Ehrenstein, and colleagues demonstrated that the ribosome recognizes the tRNA, not the amino acid, in an aminoacyl-tRNA. They did this by forming cysteyl-tRNA^{Cys}, then reducing the cysteine with Raney nickel to yield alanyl-tRNA^{Cys}, as illustrated in Figure 19.31. (Notice the nomenclature here. In cysteyl-tRNA^{Cys} [Cys-tRNA^{Cys}] the first Cys tells what amino acid is actually attached to the tRNA. The second Cys [in the superscript] tells what amino acid *should be* attached

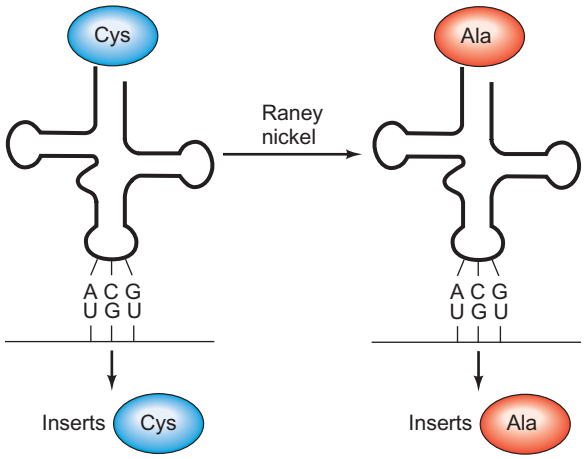

Figure 19.31 The ribosome responds to the tRNA, not the amino acid of an aminoacyl-tRNA. Lipmann, Ehrenstein, Benzer, and colleagues started with a cysteyl-tRNA^{Cys}, which inserted cysteine (Cys, blue) into a protein chain, as shown at left. They treated this aminoacyl-tRNA with Raney nickel, which reduced the cysteine to alanine (Ala, red), but had no effect on the tRNA. This alanyl-tRNA^{Cys} inserted alanine into a protein chain at a position normally occupied by cysteine, as depicted at right. Thus, the nature of the amino acid attached to the tRNA does not matter; it is the nature of the tRNA that matters, because its anticodon has to match the mRNA codon.

to this tRNA. Thus, alanyl-tRNA^{Cys} is a tRNA that *should* bind cysteine, but in this case is bound to alanine.) Then Lipmann and colleagues added this altered aminoacyl-tRNA to an in vitro translation system, along with a synthetic mRNA that was a random polymer of U and G, in a 5:1 ratio. This mRNA had many UGU codons, which encode cysteine, so it normally caused incorporation of cysteine. It should not cause incorporation of alanine because the codons for alanine are GCN, where N is any base, and the UG polymer contained no C's. However, in this case alanine was incorporated because it was attached to a tRNA^{Cys}. This showed that ribosomes do not discriminate among amino acids attached to tRNAs; they recognize only the tRNA part of an aminoacyl-tRNA.

This experiment pointed to the importance of fidelity in the aminoacyl-tRNA synthetase step. The fact that ribosomes recognize only the tRNA part of an aminoacyl-tRNA means that if the synthetases make mistakes and put the wrong amino acids on tRNAs, then these amino acids will be inserted into proteins in the wrong places. That could be very damaging because a protein with the wrong amino acid sequence is likely not to function properly. Thus, it is not surprising that aminoacyl-tRNA synthetases are very specific for the tRNAs and amino acids they bring together. This raises a major question related to the structure of tRNAs: Given that the secondary and tertiary structures of all tRNAs are essentially the same, what base sequences in tRNAs do the synthetases recognize when they are selecting one tRNA out of a pool of over 20? This set of sequences has even been dubbed the "second genetic code" to highlight its importance. This question is complicated by the fact that some **isoaccepting species** of tRNA can be charged with the same amino acid by the same synthetase, yet they have different sequences, and even different anticodons.

If we were to guess about the locations of the tRNA elements that an aminoacyl-tRNA synthetase recognizes, two sites would probably occur to us. First, the acceptor stem seems a logical choice, because that is the locus on the tRNA that accepts the amino acid and is therefore likely to lie at or near the enzyme's active site as it is being charged. Because the enzyme presumably makes such intimate contact with the acceptor stem, it should be able to discriminate among tRNAs with different base sequences in the acceptor stem. Of course, the last three bases are irrelevant for this purpose because they are the same, CCA, in all tRNAs. Second, the anticodon is a reasonable selection, because it is different in each tRNA, and it has a direct relationship to the amino acid with which the tRNA should be charged. We will see that both these predictions are correct in most cases, and some other areas of certain tRNAs also play a role in recognition by aminoacyl-tRNA synthetases.

The Acceptor Stem In 1972, Dieter Söll and his colleagues noticed a pattern in the nature of the fourth base from the 3′-end, position 73 in most tRNAs. That is, this base tended to be the same in tRNAs specific for a certain class of amino acids. For example, virtually all the hydrophobic amino acids are coupled to tRNAs with A in position 73, regardless of the species in which we find the tRNA. However, this obviously cannot be the whole story because one base does not provide enough variation to account for specific charging of 20 different classes of tRNAs. At best, it fills the role of a rough discriminator.

Bruce Roe and Bernard Dudock used another approach. They examined the base sequence of all the tRNAs from several species that could be charged by a single synthetase. This included some tRNAs that were charged with the wrong amino acid, in a process called *heterologous mischarging*. This term refers to the ability of a synthetase from one species to charge an incorrect tRNA from another species, although this mischarging is always slower and requires a higher enzyme concentration than normal. For example, yeast phenylalanyl-tRNA synthetase (PheRS) can charge tRNA^{Phe} from *E. coli,* yeast, and wheat germ correctly, but it can also charge *E. coli* tRNA^{Val} with phenylalanine.

Because all these tRNAs can be charged by the same synthetase, they should all have the elements that the synthetase uses to tell it which tRNAs to charge. So Roe and Dudock compared the sequences of all these tRNAs, looking for things they have in common, but are not common to all tRNAs. Two features stood out: base 73, and nine nucleotides in the D stem.

In 1973, J.D. Smith and Julio Celis studied a mutant suppressor tRNA that inserted Gln instead of Tyr. In other words, the wild-type suppressor tRNA was charged by the GlnRS, but some change in its sequence caused it to be charged by the TyrRS instead. The only difference between the mutant and wild-type tRNAs was a change in base 73 from G to A.

In 1988, Ya-Ming Hou and Paul Schimmel used genetic means to demonstrate the importance of a single base pair in the acceptor stem to charging specificity. They started with a tRNA^{Ala} that had its anticodon mutated to 5′-CUA-3′ so it became an amber suppressor capable of inserting alanine in response to the amber codon UAG. Then they looked for mutations in the tRNA that changed its charging specificity. Their assay was a convenient one they could run in vivo. They built a *trpA* gene with an amber mutation in codon 10. This mutation could be suppressed only by a tRNA that could insert an alanine (or glycine) in response to the amber codon. Any other amino acid in position 10 yielded an inactive protein. Finally, they challenged their mutants by growing them in the absence of tryptophan. If the mutant could suppress the amber mutation in the *trpA* gene, it had a suppressor tRNA that could still be correctly charged with alanine (or glycine). If not, the suppressor tRNA was altered so it was charged with another amino acid. They found that all the cells that grew in the absence of tryptophan had a G in position 3 of the suppressor tRNA and a U in position 70, so a G3-U70 wobble base

pair could form in the acceptor stem three bases from the end of the stem.

This experiment suggested that the G3–U70 base pair is a key determinant of charging by AlaRS. If so, these workers reasoned, they might be able to take another suppressor tRNA that inserted another amino acid, change its bases at positions 3 and 70 to G and U, respectively, and convert the charging specificity of the suppressor tRNA to alanine. They did this with two different suppressor tRNAs: $tRNA^{Cys/CUA}$ and $tRNA^{Phe/CUA}$, where the CUA designation refers to the anticodon, which recognizes the UAG amber codon. Both of the tRNAs originally had a C3–G70 base pair in their acceptor stems. However, when Hou and Schimmel changed this one base pair to G3–U70, they converted the tRNAs to $tRNA^{Ala/CUA}$, as indicated by their ability to suppress the amber mutation in codon 10 of the *trpA* gene.

Did these altered amber suppressor tRNAs really insert alanine into the TrpA protein? Amino acid sequencing revealed that they did. Furthermore, these altered tRNAs could be charged with alanine in vitro. Thus, even though these two tRNAs differed from natural $tRNA^{Ala/CUA}$ in 38 and 31 bases, respectively, changing just one base pair from C–G to G–U changed the charging specificity from Cys or Phe to Ala.

In 1989, Christopher Francklyn and Schimmel presented another line of evidence that implicates the acceptor stem, and the G3–U70 base pair in particular, in AlaRS charging specificity. They showed that a synthetic 35-nt "minihelix" resembling the top part of the inverted L-shaped $tRNA^{Ala}$, including the acceptor stem and the TΨC loop, can be efficiently charged with alanine. In fact, as long as the G3–U70 base pair was present, charging with alanine occurred even when many other bases were changed.

It is also interesting that the Ala-minihelix binds to the P site of the ribosome, and participates just as well as intact Ala-$tRNA^{Ala}$ in the peptidyl transferase reaction with puromycin. These observations have led to the speculation that the top part of the tRNA molecule evolved first, and could have participated, along with an ancestor of 23S rRNA, in a crude version of protein synthesis in the "RNA world" before ribosomes evolved.

SUMMARY Biochemical and genetic experiments have demonstrated the importance of the acceptor stem in recognition of a tRNA by its cognate aminoacyl-tRNA synthetase. In certain cases, changing one base pair in the acceptor stem can change the charging specificity.

The Anticodon In 1973, LaDonne Schulman pioneered a technique in which she treated $tRNA_f^{Met}$ with bisulfite, which converts cytosines to uracils. She and her colleagues found that many of these base alterations had no effect, but some destroyed the ability of the tRNA to be charged with methionine. One such change was a C→U change in base 73; another was a C→U change in the anticodon. Since then, Schulman and her colleagues have amassed a large body of evidence that shows the importance of the anticodon in charging specificity.

In 1983, Schulman and Heike Pelka developed a method to change specifically one or more bases at a time in the anticodon of the initiator tRNA, $tRNA_f^{Met}$. First, they cut the wild-type tRNA in two with a limited digestion with pancreatic RNase. This removed the anticodon from the tRNA 5′-fragment, and also cut off the last two nucleotides of the CCA terminus of the 3′-fragment. Then they used T4 RNA ligase to attach a small oligonucleotide to the 5′-fragment that would replace the lost anticodon, with one or more bases altered, ligated the two halves of the molecule back together, and then added back the lost terminal CA with tRNA nucleotidyltransferase. Finally, they tested the tRNAs with altered anticodons in charging reactions in vitro. Table 19.1 shows that changing one base in the anticodon of $tRNA_f^{Met}$ was sufficient to lower the rate of charging with Met by at least a factor of 10^5. The first base in the anticodon (the "wobble" position) was the most sensitive; changing this one base always had

Table 19.1 Initial Rates of Aminoacylation of $tRNA_f^{Met}$ Derivatives

tRNA*	Mol Met-tRNA/mol Met-tRNA synthetase per min	Relative rate, CAU/other
$tRNA_f^{Met}$	28.45	0.8
$tRNA_f^{Met}$ (gel)†	22.80	1
CAU	22.15	1
CAUA	1.59	14
CCU	4.0×10^{-1}	55
CUU	2.6×10^{-2}	850
CUA	2.0×10^{-2}	1100
CAG	1.7×10^{-2}	1300
CAC	1.2×10^{-3}	18,500
CA	0.5×10^{-3}	44,000
C	$<10^{-4}$	$>10^5$
ACU	$<10^{-4}$	$>10^5$
UAU	$<10^{-4}$	$>10^5$
AAU	$<10^{-4}$	$>10^5$
GAU	$<10^{-4}$	$>10^5$

*The oligonucleotide inserted in the anticodon loop of synthesized $tRNA_f^{Met}$ derivatives is indicated.
†Control sample isolated from a denaturing polyacrylamide gel in parallel with the synthesized $tRNA_f^{Met}$ derivatives.
Source: L.H. Schulman and H. Pelka, "Anticodon Loop Size and Sequence Requirements for Recognition of Formylmehionine tRNA by Methionyl-tRNA Synthetase," *Proceedings of the National Academy of Sciences,* November 1983. Reprinted with permission of the author.

a drastic effect on charging. Thus, the anticodon seems to be required for charging of this tRNA in vitro.

In 1991, Schulman and Leo Pallanck followed up the earlier in vitro studies with an in vivo study of the effects of altering the anticodon. Again, they changed the anticodon of the $tRNA_f^{Met}$, but this time they tested the ability of the altered tRNA to be mischarged with the amino acid corresponding to the new anticodon. They tested mischarging with a reporter gene encoding dihydrofolate reductase (DHFR), which is easy to isolate in highly purified form. Here is an example of how the assay worked: They altered the gene for $tRNA_f^{Met}$ so its anticodon was changed from CAU to GAU, which is an isoleucine (Ile) anticodon. Then they placed this mutant gene into *E. coli* cells, along with a mutant DHFR gene bearing an AUC initiation codon.

Ordinarily, AUC would not work well as an initiation codon, but in the presence of a $tRNA_f^{Met}$ with a complementary anticodon, it did. Sequencing of the resulting DHFR protein demonstrated that the amino acid in the first position was primarily Ile. Some Met occurred in the first position, showing that the endogenous wild-type $tRNA_f^{Met}$ could recognize the AUC initiation codon to some extent.

Pallanck and Schulman used the same procedure to change the $tRNA_f^{Met}$ anticodon to GUC (valine, Val) or UUC (phenylalanine, Phe). In each case, they made a corresponding change in the DHFR initiation codon so it was complementary to the anticodon in the altered $tRNA_f^{Met}$. In both cases, the gene functioned significantly better in the presence than in the absence of the complementary $tRNA_f^{Met}$. More importantly, this experiment showed that the nature of the initiating amino acid can change with the alteration in the tRNA anticodon. In fact, with the $tRNA_f^{Met}$ bearing the valine anticodon, valine was the only amino acid found at the amino terminus of the DHFR protein. This means that a change of the $tRNA_f^{Met}$ anticodon from CAU to GAC altered the charging specificity of this tRNA from methionine to valine. Thus, in this case, the anticodon seems to be the crucial factor in determining the charging specificity of the tRNA.

On the other hand, changing the anticodon of the $tRNA_f^{Met}$ always reduced its efficiency. In fact, most such alterations yielded $tRNA_f^{Met}$ molecules whose efficiency was too low to analyze further, even in the presence of complementary initiation codons. Thus, some aminoacyl-tRNA synthetases could charge a noncognate tRNA with an altered anticodon, but others could not. These latter enzymes apparently required more cues than just the anticodon.

SUMMARY Biochemical and genetic experiments have shown that the anticodon, like the acceptor stem, is an important element in charging specificity. Sometimes the anticodon can be the absolute determinant of specificity.

Structures of Synthetase–tRNA Complexes X-ray crystallography studies of complexes between tRNAs and their cognate aminoacyl-tRNA synthetases have shown that both the acceptor stem and the anticodon have docking sites on the synthetases. Thus, these findings underline the importance of the acceptor stem and anticodon in synthetase recognition. In 1989, Dieter Söll and Thomas Steitz and their colleagues used x-ray crystallography to determine the first three-dimensional structure of an aminoacyl-tRNA synthetase (*E. coli* GlnRS) bound to its cognate tRNA. Figure 19.32 presents this structure. Near the top, we see a deep cleft in the enzyme that enfolds the acceptor stem, including base 73 and the 3–70 base pair. At lower left, we observe a smaller cleft in the enzyme into which the anticodon of the tRNA protrudes. This would allow for

Figure 19.32 Three-dimensional structure of glutaminyl-tRNA synthetase complexed with tRNA and ATP. The synthetase is shown in blue, the tRNA in brown and yellow, and the ATP in green. Note the three areas of contact between enzyme and tRNA: (1) the deep cleft at top that holds the acceptor stem of the tRNA, and the ATP; (2) the smaller pocket at lower left into which the tRNA's anticodon inserts; and (3) the area in between these two clefts, which contacts much of the inside of the L of the tRNA. (*Source:* Courtesy T.A. Steitz; from Rould, Perona, Vogt, and Steitz, *Science* 246 (1 Dec 1989) cover. Copyright © AAAS.)

specific recognition of the anticodon by the synthetase. In addition, we see that most of the left side of the enzyme is in intimate contact with the inside of the L of the tRNA, which includes the D loop side and the minor groove of the acceptor stem.

About half the synthetases, including GlnRS, are in a group called **class I.** These are all structurally similar and initially aminoacylate the 2′-hydroxyl group of the terminal adenosine of the tRNA. The other half of the synthetases are in **class II;** they are structurally similar to other members of their group, but quite different from the members of class I, and they initially aminoacylate the 3′-hydroxyl group of their cognate tRNAs. In 1991, D. Moras and colleagues obtained the x-ray crystal structure of a member of this group, yeast AspRS, together with $tRNA^{Asp}$. Figure 19.33 contrasts the structures of the class I and class II synthetase–tRNA complexes. Several differences stand out. First, although the synthetase still contacts the inside of the L, it does so on the tRNA's opposite face, including the variable loop and the major groove of the acceptor stem.

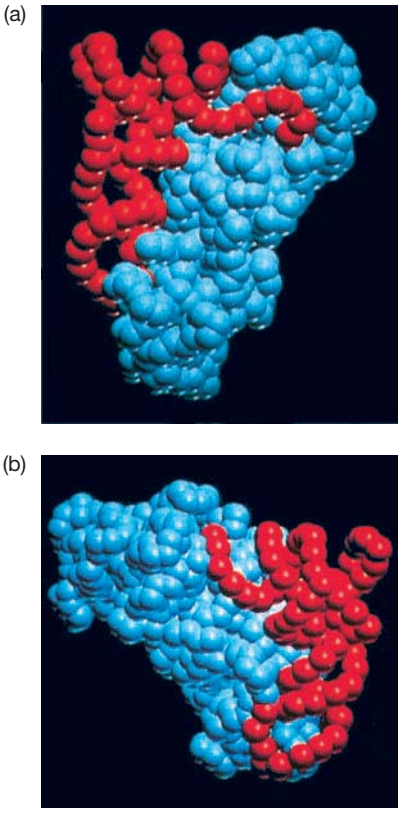

Figure 19.33 Models of (a) a class I complex: *E. coli* GlnRS-$tRNA^{Gln}$, and (b) a class II complex: yeast AspRS-$tRNA^{Asp}$. For simplicity, only the phosphate backbones of the tRNAs (red) and the α-carbon backbones of the synthetases (blue) are shown. Notice the approach of the two synthetases to the opposite sides of their cognate tRNAs. (*Source:* Ruff, M., S. Krishnaswamy, M. Boeglin, A. Poterszman, A. Mitschler, A. Podjarny, B. Rees, J.C. Thierry, and D. Moras, Class II aminoacyl transfer RNA synthetases: Crystal structure of yeast aspartyl-tRNA synthetase complexed with $tRNA^{Asp}$. *Science* 252 (21 June 1991) f. 3, p. 1686. Copyright © AAAS.)

Also, the acceptor stem, including the terminal CCA, is in a regular helical conformation. This contrasts with the class I structure, in which the first base pair is broken and the 3′-end of the molecule makes a hairpin turn. Thus, x-ray crystallography has corroborated the major conclusions of biochemical and genetic studies on synthetase–tRNA interactions: Both the anticodon and acceptor stem are in intimate contact with the enzyme and are therefore in a position to determine specificity of enzyme–tRNA interactions.

SUMMARY X-ray crystallography has shown that synthetase–tRNA interactions differ between the two classes of aminoacyl-tRNA synthetases. Class I synthetases have pockets for the acceptor stem and anticodon of their cognate tRNAs and approach the tRNAs from the D loop and acceptor stem minor groove side. Class II synthetases also have pockets for the acceptor stem and anticodon, but approach their tRNAs from the opposite side, which includes the variable arm and major groove of the acceptor stem.

Proofreading and Editing by Aminoacyl-tRNA Synthetases

As good as aminoacyl-tRNA synthetases are at recognizing the correct (cognate) tRNAs, they have a more difficult job recognizing the cognate amino acids. The reason is clear: tRNAs are large, complex molecules that vary from one another in nucleotide sequence and in nucleoside modifications, but amino acids are simple molecules that resemble one another fairly closely—sometimes very closely. Consider isoleucine and valine, for example. The two amino acids are identical except for an extra methylene (CH_2) group in isoleucine. In 1958, Linus Pauling used thermodynamic considerations to calculate that isoleucyl-tRNA synthetase (IleRS) should make about one-fifth as much incorrect Val-$tRNA^{Ile}$ couples as correct Ile-$tRNA^{Ile}$ couples. In fact, however, only one in 150 amino acids activated by IleRS is valine, and only one in 3000 aminoacyl-tRNAs produced by this enzyme is Val-$tRNA^{Ile}$. How does isoleucyl-tRNA synthetase prevent formation of Val-$tRNA^{Ile}$?

As first proposed by Alan Fersht in 1977, the enzyme uses a *double-sieve* mechanism to avoid producing tRNAs with the wrong amino acid attached. Figure 19.34 illustrates this concept. The first sieve is accomplished by the **activation site** of the enzyme, which rejects substrates that are too large. However, substrates such as valine that are too small can fit into the activation site and so get activated to the aminoacyl adenylate form and sometimes make it all the way to the aminoacyl-tRNA form. That is where the second sieve comes into play. Activated amino acids or, less

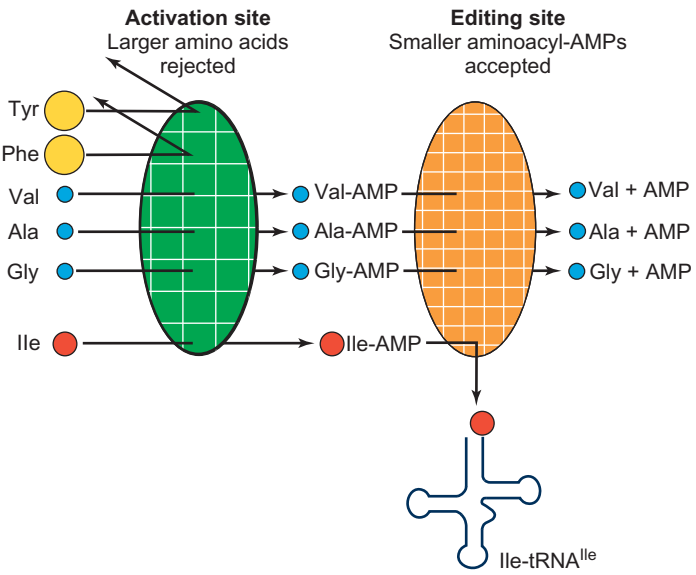

Figure 19.34 The double sieve of isoleucine-tRNA synthetase. The activation site is the coarse sieve in which large amino acids, such as Tyr and Phe, are excluded because they don't fit. The editing (hydrolytic) site is the fine sieve, which accepts activated amino acids smaller than Ile-AMP, such as Val-AMP, Ala-AMP, and Gly-AMP, but rejects Ile-AMP because it is too large. As a result, the smaller activated amino acids are hydrolyzed to AMP and amino acids, whereas Ile-AMP is converted to Ile-tRNA^{Ile}. (*Source:* Adapted from Fersht, A.R., Sieves in sequence. *Science* 280:541, 1998.)

commonly, aminoacyl-tRNAs that are too small are hydrolyzed by another site on the enzyme: the **editing site.**

For example, IleRS uses the first sieve to exclude amino acids that are too large, or the wrong shape. Thus, the enzyme excludes phenylalanine because it is too large and leucine because it is the wrong shape. (One of the terminal methyl groups of leucine cannot fit into the activation site.) But what about smaller amino acids such as valine? In fact, they do fit into the activation site of IleRS, and so they become activated. But then they are transported to the editing site, where they are recognized as incorrect and deactivated. This second sieve is called either **proofreading** or **editing.**

Shigeyuki Yokoyama and colleagues have obtained the crystal structure of the *T. thermophilus* IleRS alone, coupled to its cognate amino acid, isoleucine, and to the noncognate amino acid valine. These structures have amply verified Fersht's elegant hypothesis. Figure 19.35 shows the structure of the activation site, with either (a) isoleucine, or (b) valine bound. We can see that both amino acids fit well into this site, although valine makes slightly weaker contact with two of the hydrophobic amino acid side chains (Pro46 and Trp558) that surround the site. On the other hand, it is clear that this site is too small to admit large amino acids such as phenylalanine, and even leucine would be sterically hindered from binding by one of its two terminal methyl groups. This picture is fully consistent with the coarse sieve part of the double-sieve hypothesis.

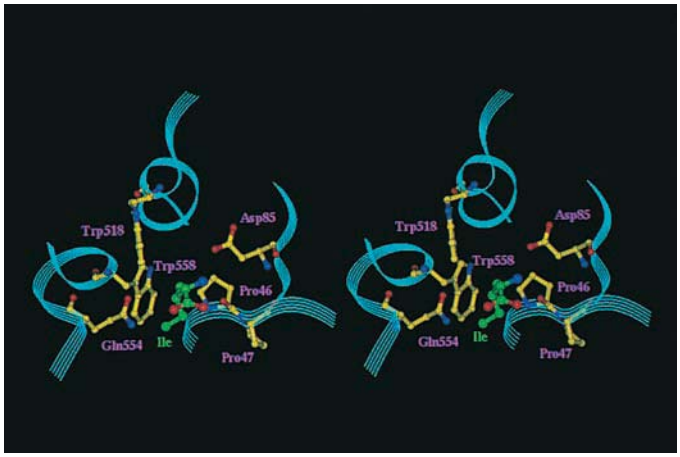

(a)

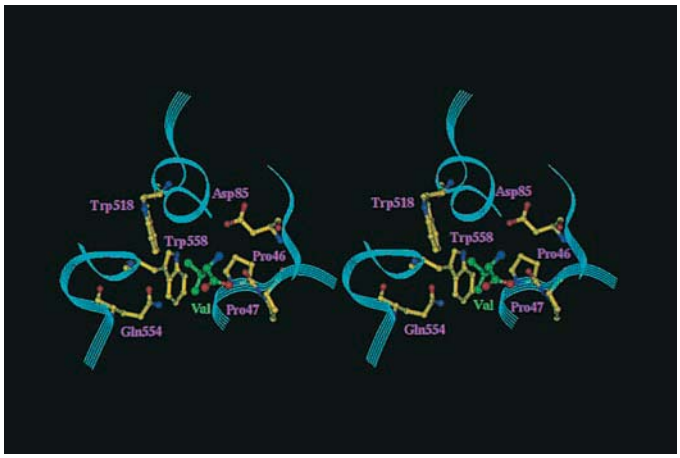

(b)

Figure 19.35 Stereo views of isoleucine and valine in the activation site of IleRS. The backbone of the enzyme is represented by turquoise ribbons, with the carbons of amino acid side chains in yellow. The carbons of the substrates [isoleucine **(a),** valine **(b)**] are rendered in green. Oxygens of all amino acids are in red and nitrogens are in blue. Note that both isoleucine and valine fit into the activation site. (*Source:* Nureki, O., D.G. Vassylyev, M. Tateno, A. Shimada, T. Nakama, S. Fukai, M. Konno, T.L. Henrickson, P. Schimmel, and S. Yokoyama, Enzyme structure with two catalytic sites for double-sieve selection of substrate. *Science* 280 (24 Apr 1998) f. 2, p. 579. Copyright © AAAS.)

The enzyme has a second deep cleft comparable in size to the cleft of the activation site, but 34 Å away. This second cleft is thought to be the editing site, based in part on the fact that a fragment of the enzyme containing this cleft still retains editing activity. The crystal structure confirms this hypothesis: When Yokoyama and colleagues prepared crystals of the IleRS with valine, they found a molecule of valine at the bottom of the deep cleft. However, when they prepared crystals with isoleucine, no amino acid was found in the cleft. Thus, because the cleft seems to be specific for valine, it appears to be the editing site. Furthermore, inspection of the pocket in which valine is found, shows that the space in between the side chains of Trp232 and Tyr386

is just big enough to accommodate valine, but too small to admit isoleucine.

If this really is the editing site, we would expect that its removal would abolish editing. Indeed, when Yokoyama and colleagues removed 47 amino acids from this region, including Trp232, they abolished editing activity while retaining full activation activity. Thus, the second cleft really does appear to be the editing site. Several amino acid side chains are particularly close to the valine in the cleft, and Thr230 and Asn237 are well-positioned to take part in the hydrolysis reaction that is the essence of editing. To test this hypothesis, Yokoyama and coworkers changed the amino acids in the *E. coli* IleRS (Thr243 and Asn250) that correspond to Thr230 and Asn237 in the *T. thermophilus* enzyme. Sure enough, when they changed these two amino acids to alanine, the enzyme lost its editing activity, but retained its activation activity. All these data are consistent with the hypothesis that the second cleft is the editing site, and that hydrolysis of noncognate aminoacyl-AMPs such as Val-AMP occurs there.

SUMMARY The amino acid selectivity of at least some aminoacyl-tRNA synthetases is controlled by a double-sieve mechanism. The first sieve is a coarse one that excludes amino acids that are too big. The enzyme accomplishes this task with an active site for activation of amino acids that is just big enough to accommodate the cognate amino acid, but not larger amino acids. The second sieve is a fine one that degrades aminoacyl-AMPs that are too small. The enzyme accomplishes this task with a second active site (the editing site) that admits small aminoacyl-AMPs and hydrolyzes them. The cognate aminoacyl-AMP is too big to fit into the editing site, so it escapes being hydrolyzed. Instead, the enzyme transfers the activated amino acid to its cognate tRNA.

SUMMARY

X-ray crystallography studies on bacterial ribosomes with and without tRNAs have shown that the tRNAs occupy the cleft between the two subunits. They interact with the 30S subunit through their anticodon ends, and with the 50S subunit through their acceptor stems. The binding sites for the tRNAs are composed primarily of rRNA. The anticodons of the tRNAs in the A and P sites approach each other closely enough to base-pair with adjacent codons in the mRNA bound to the 30S subunit, given that the mRNA kinks 45 degrees between the two codons. The acceptor stems of the tRNAs in the A and P sites also approach each other closely—within just 5 Å—in the peptidyl transferase pocket of the 50S subunit. Twelve contacts between ribosomal subunits are visible.

The crystal structure of the *E. coli* ribosome contains two structures that differ from each other by rigid body motions of domains of the ribosome, relative to each other. In particular, the head of the 30S particle rotates by 6 degrees, and by 12 degrees compared to the *T. thermophilus* ribosome. This rotation is probably part of the ratchet action of the ribosome that occurs during translocation.

The *E. coli* 30S subunit contains a 16S rRNA and 21 proteins (S1–S21). The 50S subunit contains a 5S rRNA, a 23S rRNA, and 34 proteins (L1–L34). Eukaryotic cytoplasmic ribosomes are larger and contain more RNAs and proteins than their prokaryotic counterparts.

Sequence studies of 16S rRNA led to a proposal for the secondary structure (intramolecular base pairing) of this molecule. X-ray crystallography studies have confirmed the conclusions of these studies. They show a 30S subunit with an extensively base-paired 16S rRNA whose shape essentially outlines that of the whole particle. The x-ray crystallography studies have also confirmed the locations of most of the 30S ribosomal proteins.

The 30S ribosomal subunit plays two roles. It facilitates proper decoding between codons and aminoacyl-tRNA anticodons, including proofreading. It also participates in translocation. Crystal structures of the 30S subunit with three antibiotics that interfere with these two roles shed light on translocation and decoding. Spectinomycin binds to the 30S subunit near the neck, where it can interfere with the movement of the head that is required for translocation. Streptomycin binds near the A site of the 30S subunit and stabilizes the *ram* state of the ribosome. This reduces fidelity of translation by allowing noncognate aminoacyl-tRNAs to bind relatively easily to the A site and by preventing the shift to the restrictive state that is necessary for proofreading. Paromomycin binds in the major groove of the 16S rRNA H44 helix near the A site. This flips out bases A1492 and A1493, so they can stabilize base-pairing between codon and anticodon, including anticodons on noncognate aminoacyl-tRNAs, so fidelity declines.

The x-ray crystal structure of IF1 bound to the 30S ribosomal subunit shows that IF1 binds to the A site. In that position, it clearly blocks fMet-tRNA from binding to the A site, and may also actively promote fMet-tRNA binding to the P site through a presumed interaction between IF1 and IF2. IF1 also interacts intimately with helix H44 of the 30S subunit, and this may explain how IF1 accelerates both association and dissociation of the ribosomal subunits.

The crystal structure of the 50S ribosomal subunit has been determined to 2.4 Å resolution. This structure reveals relatively few proteins at the interface between ribosomal

subunits, and no protein within 18 Å of the peptidyl transferase active center tagged with a transition state analog. The 2′-OH group of the tRNA in the P site is very well positioned to form a hydrogen bond to the amino group of the aminoacyl-tRNA in the A site, and therefore to help catalyze the peptidyl transferase reaction. In accord with this hypothesis, removal of this hydroxyl group eliminates almost all peptidyl transferase activity. Similarly, removal of the 2′-OH group of A2451 of the 23S rRNA strongly inhibits peptidyl transferase activity. This group may also participate in catalysis by hydrogen bonding, or it may help position the reactants properly for catalysis. The exit tunnel through the 50S subunit is just wide enough to allow a protein α-helix to pass through. Its walls are made of RNA, whose hydrophilicity is likely to allow exposed hydrophobic side chains of the nascent polypeptide to slide through easily. RF1 domains 2 and 3 fill the codon recognition site and the peptidyl transferase site, respectively, of the ribosome's A site, in recognizing the UAA stop codon. The "reading head" portion of domain 2 of RF1, including its conserved PXT motif, occupies the decoding center within the A site and collaborates with A1493 and A1492 of the 16S rRNA to recognize the stop codon. The universally conserved GGQ motif at the tip of domain 3 of RF1 closely approaches the peptidyl transferase center and participates in cleavage of the ester bond linking the completed polypeptide to the tRNA. RF2 binds to the ribosome and operates in much the same way in response to the UGA stop codon.

Most mRNAs are translated by more than one ribosome at a time; the result, a structure in which many ribosomes translate an mRNA in tandem, is called a polysome. In eukaryotes, polysomes are found in the cytoplasm. In prokaryotes, transcription of a gene and translation of the resulting mRNA occur simultaneously. Therefore, many polysomes are found associated with an active gene.

Transfer RNA was discovered as a small RNA species independent of ribosomes that could be charged with an amino acid and could then pass the amino acid to a growing polypeptide. All tRNAs share a common secondary structure represented by a cloverleaf. They have four base-paired stems defining three stem loops (the D loop, anticodon loop, and T loop) and the acceptor stem, to which amino acids are added in the charging step. The tRNAs also share a common three-dimensional shape that resembles an inverted L. This shape maximizes stability by lining up the base pairs in the D stem with those in the anticodon stem, and the base pairs in the T stem with those in the acceptor stem. The anticodon of the tRNA protrudes from the side of the anticodon loop and is twisted into a shape that readily base-pairs with the corresponding codon in mRNA.

The acceptor stem and anticodon are important cues in recognition of a tRNA by its cognate aminoacyl-tRNA synthetase. In certain cases, each of these elements can be the absolute determinant of charging specificity. X-ray crystallography has shown that synthetase–tRNA interactions differ between the two classes of aminoacyl-tRNA synthetases. Class I synthetases have pockets for the acceptor stem and anticodon of their cognate tRNAs and approach the tRNAs from the D loop and acceptor stem minor groove side. Class II synthetases also have pockets for the acceptor stem and anticodon, but approach their tRNAs from the opposite side, which includes the variable arm and major groove of the acceptor stem.

The amino acid selectivity of at least some aminoacyl-tRNA synthetases is controlled by a double-sieve mechanism. The first sieve is a coarse one that excludes amino acids that are too big. The enzyme accomplishes this task with an active site for activation of amino acids that is just big enough to accommodate the cognate amino acid, but not larger amino acids. The second sieve is a fine one that degrades aminoacyl-AMPs that are too small. The enzyme accomplishes this task with a second active site (the editing site) that admits small aminoacyl-AMPs and hydrolyzes them. The cognate aminoacyl-AMP is too big to fit into the editing site, so it escapes being hydrolyzed.

REVIEW QUESTIONS

1. Draw rough sketches of the *E. coli* 30S and 50S ribosomal subunits and show how they fit together to form a 70S ribosome.
2. Draw rough sketches of interface views of both 50S and 30S ribosomal subunits. Point out the rough positions of tRNAs in the A, P, and E sites.
3. What parts of the tRNAs interact with the 30S subunit? With the 50S subunit?
4. Why is it important that the anticodons of the tRNAs in the A and P sites approach each other closely?
5. Why is it important that the acceptor stems of the tRNAs in the A and P sites approach each other closely?
6. Describe the process of two-dimensional gel electrophoresis described in this chapter. In what way is two-dimensional superior to one-dimensional electrophoresis?
7. Present plausible hypotheses to explain how the following antibiotics interfere with translation. Present evidence for each hypothesis.
   a. Streptomycin
   b. Paromomycin
8. How can x-ray diffraction data rule out ribosomal proteins as the active site in peptidyl transferase?
9. Outline the evidence for the importance of the 2′-OH of the terminal adenosine of the peptidyl-tRNA in the P site in transpeptidation. How is this hydroxyl group likely to participate in transpeptidation?

10. Outline the evidence for the importance of the 2′-OH of A2451 of the 23S rRNA in transpeptidation. How is this hydroxyl group likely to participate in transpeptidation?
11. How do we know the base of A2451 (A2486 in *H. marismortui*) is not important in transpeptidation?
12. What part of RF1 recognizes the stop codon UAA? What ribosomal elements participate in this recognition? What part of RF1 participates in cleavage of the bond between the tRNA and the peptide?
13. Explain how the bending of the tRNA in an aminoacyl-tRNA as it first binds to the A site (actually the A/T site), and the unbending of the tRNA during accommodation in the A site, contribute to accuracy of translation.
14. Describe the experiments that led to the discovery of tRNA.
15. How was the "cloverleaf" secondary structure of tRNA discovered?
16. Draw the cloverleaf tRNA structure and point out the important structural elements.
17. Describe and give the results of an experiment that shows that the ribosome responds to the tRNA part, not the amino acid part, of an aminoacyl-tRNA.
18. Describe and give the results of an experiment that shows that the G3–U70 base pair in a tRNA acceptor stem is a key determinant in the charging of the tRNA with alanine.
19. Present at least one line of evidence for the importance of the anticodon in the recognition of a tRNA by an aminoacyl-tRNA synthetase.
20. Based on x-ray crystallographic studies, what parts of a tRNA are in contact with the cognate aminoacyl-tRNA synthetase?
21. Diagram a double-sieve mechanism that ensures amino acid selectivity in aminoacyl-tRNA synthetases.
22. Outline the evidence for the double sieve in the isoleucine–tRNA synthetase that excludes larger and smaller amino acids.

ANALYTICAL QUESTIONS

1. Draw a diagram of a hypothetical eukaryotic polysome in which nascent protein chains are visible. Identify the 5′- and 3′-ends of the mRNA and use an arrow to indicate the direction the ribosomes are moving along the mRNA. Use N and C to indicate the amino and carboxyl ends of one of the growing polypeptides.
2. Draw a diagram of a hypothetical prokaryotic gene being transcribed and translated simultaneously. Show the nascent mRNAs with ribosomes attached, but do not show nascent proteins. With an arrow, indicate the direction of transcription.
3. You are investigating a $tRNA^{Phe}$ whose charging specificity appears to be affected by a C11–G24 base pair in the D stem. Design two experiments to show that changing this base pair changes the charging specificity of the tRNA. The first experiment should be a biochemical one using an in vitro reaction. The second should be a genetic one performed in vivo.
4. Consider the process of bringing a new aminoacyl-tRNA to the A site, as revealed by x-ray crystallography. Describe the probable effects of each of the following mutations on speed and fidelity of translation:
   a. A mutation in the 16S rRNA that facilitates "domain closure" in the 30S subunit.
   b. A mutation in the acceptor stem of the tRNA that inhibits the change in conformation that normally helps the tRNA bend into the A/T state.
   c. A mutation in switch I of EF-Tu that strengthens its binding to the acceptor stem of tRNA.
   d. Mutating His 84 of EF-Tu to Alanine.

SUGGESTED READINGS

General References and Reviews

Cech, T.R. 2000. The ribosome is a ribozyme. *Science* 289:878–79.
Dahlberg, A.E. 2001. The ribosome in action. *Science* 292:868–69.
Fersht, A.R. 1998. Sieves in sequence. *Science* 280:541.
Liljas, A. 2009. Leaps in translation elongation. *Science* 326:677–78.
Moore, P.B. 2005. A ribosomal coup: *E. coli* at last! *Science* 310:793–95.
Noller, H.F. 1990. Structure of rRNA and its functional interactions in translation. In Hill, W.E., et al., eds. *The Ribosome: Structure, Function and Evolution.* Washington, D.C.: American Society for Microbiology, chapter 3, pp. 73–92.
Pennisi, E. 2001. Ribosome's inner workings come into sharper view. *Science* 291:2526–27.
Saks, M.E., J.R. Sampson, and J.N. Abelson. 1994. The transfer RNA identity problem: A search for rules. *Science* 263:191–97.
Schmeing, T.M. and V. Ramakrishnan. 2009. What recent ribosome structures have revealed about the mechanism of translation. *Nature* 461:1234–42.
Waldrop, M.M. 1990. The structure of the "second genetic code." *Science* 246:1122.

Research Articles

Ban, N., P. Nissen, J. Hansen, P.B. Moore, and T.A. Steitz. 2000. The complete atomic structure of the large ribosomal subunit at 2.4 Å resolution. *Science* 289:905–20.
Carter, A.P., W.M. Clemons, Jr., D.E. Brodersen, R.J. Morgan-Warren, T. Hartsch, B.T. Wimberly, and V. Ramakrishnan. 2000. Crystal structure of an initiation factor bound to the 30S ribosomal subunit. *Science* 291:498–501.
Carter, A.P., W.M. Clemons, Jr., D.E. Brodersen, R.J. Morgan-Warren, T. Hartsch, B.T. Wimberly, and V. Ramakrishnan. 2000. Functional insights from the structure of the 30S

ribosomal subunit and its interactions with antibiotics. *Nature* 407:340–48.

Gao, Y.-G., M. Selmer, C.M. Dunham, A. Weixlbaumer, A.C. Kelley, and V. Ramakrishnan. 2009. The structure of the ribosome with elongation factor G trapped in the posttranslocation state. *Science* 326:694–99.

Hoagland, M.B., M.L. Stephenson, J.F. Scott, L.I. Hecht, and P.C. Zamecnik. 1958. A soluble ribonucleic acid intermediate in protein synthesis. *Journal of Biological Chemistry* 231:241–57.

Holley, R.W., J. Apgar, G.A. Everett, J.T. Madison, M. Marquisee, S.H. Merrill, J.R. Penswick, and A. Zamir. 1965. Structure of a ribonucleic acid. *Science* 147:1462–65.

Kaltschmidt, E. and H.G. Wittmann. 1970. Ribosomal proteins XII: Number of proteins in small and large ribosomal subunits of *Escherichia coli* as determined by two-dimensional gel electrophoresis. *Proceedings of the National Academy of Sciences USA* 67:1276–82.

Kim, S.H., F.L. Suddath, G.J. Quigley, A. McPherson, J.L. Sussman, A.H.J. Wang, N. C. Seeman, and A. Rich. 1974. Three-dimensional tertiary structure of yeast phenylalanine transfer RNA. *Science* 185:435–40.

Lake, J.A. 1976. Ribosome structure determined by electron microscopy of *Escherichia coli* small subunits, large subunits and monomeric ribosomes. *Journal of Molecular Biology* 105:131–59.

Laurberg, M., H. Asahara, A. Korostelev, J. Zhu, S. Trakhanov, and H.F. Noller. 2008. Structural basis for translation termination on the 70S ribosome. *Nature* 454:852–57.

Miller, O., B.A. Hamkalo, and C.A. Thomas, Jr. 1970. Visualization of bacterial genes in action. *Science* 169:392–95.

Mizushima, S. and M. Nomura. 1970. Assembly mapping of 30S ribosomal proteins from *E. coli*. *Nature* 226:1214–18.

Muth, G.W., L. Ortoleva-Donnelly, and S.A. Strobel. 2000. A single adenosine with a neutral pK_a in the ribosomal peptidyl transferase center. *Science* 289:947–50.

Nissen, P., J. Hansen, N. Ban, P.B. Moore, and T.A. Steitz. 2000. The structural basis of ribosome activity in peptide bond synthesis. *Science* 289:920–30.

Nureki, O., D.G. Vassylyev, M. Tateno, A. Shimada, T. Nakama, S. Fukai, M. Konno, T.L. Henrickson. P. Schimmel, and S. Yokoyama. 1998. Enzyme structure with two catalytic sites for double-sieve selection of substrates. *Science* 280:578–82.

Ogle, J.M., D.E Brodersen, W.M.Clemons Jr., M.J. Tarry, A.P. Carter, and V. Ramakrishnan. 2001. Recognition of cognate transfer RNA by the 30S ribosomal subunit. *Science* 292:897–902.

Polacek, N., M. Gaynor, A. Yassin, and A.S Mankin. 2001. Ribosomal peptidyl transferase can withstand mutations at the putative catalytic nucleotide. *Nature* 411:498–501.

Quigley, G.J. and A. Rich. 1976. Structural domains of transfer RNA molecules. *Science* 194:796–806.

Rould, M.A., J.J. Perona, D. Söll, and T.A. Steitz. 1989. Structure of *E. coli* glutaminyl-tRNA synthetase complexed with $tRNA^{Gln}$ and ATP at 2.8 Å resolution. *Science* 246:1135–42.

Ruff, M., S. Krishnaswamy, M. Boeglin, A. Poterszman, A. Mitschler, A. Podjarny, B. Rees, J.C. Thierry, and D. Moras. 1991. Class II aminoacyl transfer RNA synthetases: Crystal structure of yeast aspartyl-tRNA synthetase complexed with $tRNA^{Asp}$. *Science* 252:1682–89.

Schluenzen, F., A. Tocilj, R. Zarivach, J. Harms, M. Gluehmann, D. Janell, A. Bashan, H. Bartels, I. Agmon, F. Franceschi, and A. Yonath. 2000. Structure of functionally activated small ribosomal subunit at 3.3 Å resolution. *Cell* 102:615–23.

Schmeing, T.M., R.M. Voorhees, A.C. Kelley, Y.-G. Gao, F.V. Murphy IV, J.R. Weir, and V. Ramakrishnan. 2009. The crystal structure of the ribosome bound to EF-Tu and aminoacyl-tRNA. *Science* 326:688–94.

Schulman, L.H. and H. Pelka. 1983. Anticodon loop size and sequence requirements for recognition of formylmethionine tRNA by methionyl-tRNA synthetase. *Proceedings of the National Academy of Sciences USA* 80:6755–59.

Schuwirth, B.S., M.A. Borovinskaya, C.W. Hau, W. Zhang, A. Vila-Sanjurjo, J.M. Holton, and J.H. Doundna Cate. 2005. Structures of the bacterial ribosome at 3.5 Å resolution. *Science* 310:827–34.

Stern, S., B. Weiser, and H.F. Noller. 1988. Model for the three-dimensional folding of 16S ribosomal RNA. *Journal of Molecular Biology* 204:447–81.

Weinger, J.S., K.M. Parnell, S. Dorner, R. Green, and S.A. Strobel. 2004. Substrate-assisted catalysis of peptide bond formation by the ribosome. *Nature Structural and Molecular Biology* 11:1101–06.

Wimberly, B.T., D.E. Brodersen, W.M. Clemons Jr., R.J. Morgan-Warren, A.P. Carter, C. Vonrhein, T. Hartsch, and V. Ramakrishnan. 2000. Structure of the 30S ribosomal subunit. *Nature* 407:327–39.

Yusupov, M.M., G. Zh. Yusupova, A. Baucom, K. Lieberman, T.N. Earnest, J.H.D. Cate, and H.F Noller. 2001. Crystal structure of the ribosome at 5.5 Å resolution. *Science* 292:883–96.